2009

A novel antibody based capture matrix utilizing human serum albumin and streptococcal Protein G to increase capture efficiency of bacteria

Christie Renee McCabe
University of South Florida

A Novel Antibody Based Capture Matrix Utilizing Human Serum Albumin and Streptococcal Protein G to Increase Capture Efficiency of Bacteria

by

Christie Renee McCabe

A thesis submitted in partial fulfillment
of the requirements for the degree of
Master of Science
Department of Cellular Microbiology and Molecular Biology
College of Arts and Sciences
University of South Florida

Major Professor: Daniel V. Lim, Ph.D.
Lindsey N. Shaw, Ph.D.
My Lien Dao, Ph.D.

Date of Approval:
April 7, 2009

Keywords: ELISA, RAPTOR, biosensor, waveguide, immobilization, detection, *Escherichia coli* O157:H7, orientation

DEDICATION

To my family, for their words of encouragement and their works of courage; without them you wouldn't be reading this. To the loves of my life Sam, Mom, Julie, John, and Joal; thank you for lifting me up when I fell, making me laugh when it wasn't funny, and protecting our country. With such inspiration all things are possible.

ACKNOWLEDGEMENTS

Thanks to Sonia Magana, Sarah Schlemmer, Dawn Hunter and Sonja Dickey at the Advanced Biosensors Laboratory, for incredible technical assistance, strategic advice, and fun conversations. Thanks also to Dr. Harvey George, and Joseph Peppe, at the Massachusetts Department of Public Health State Laboratory Institute, for their kind donation of the *E. coli* O157:H7 strain used in this study. Special thanks to Dr. Joyce Stroot for developing the capture efficiency procedure. Eternal gratitude belongs to Dr. Betty Kearns for her gentle guidance, and tireless support. Appreciation is extended to my committee members: Dr. MyLien Dao for fostering confidence in me, and to Dr. Lindsey Shaw for sharing his authoring expertise with me. Ultimately, I would like to thank Dr. Daniel Lim for believing in my idea, providing opportunities for success, and for being an extraordinary mentor.

TABLE OF CONTENTS

LIST OF TABLES

LIST OF FIGURES

A NOVEL ANTIBODY BASED CAPTURE MATRIX

UTILIZING HUMAN SERUM ALBUMIN AND STREPTOCOCCAL PROTEIN G

TO INCREASE CAPTURE EFFICIENCY OF BACTERIA

CHRISTIE RENEE MCCABE

ABSTRACT

A novel capture matrix utilizing human serum albumin (HSA) and streptococcal Protein G (PG), which possesses an albumin binding domain (ABD), was used to immobilize antibodies for improved bacterial capture efficiency in immunoassays. Enzyme linked immunosorbent assays (ELISA) were used to characterize and optimize a specific protocol for the HSA-PG capture matrix; which revealed several critical factors that should be considered. The Fc binding domain, on PG, should have high affinity for the species of capture antibody used in the assay. Goat and rabbit species antibodies bound strongly to the Fc binding domain of PG. Displacement of the capture antibody, by the detector antibody should be avoided to reduce background signals. The Fc binding domain on PG should have equivalent or lower affinity for the detector antibody, when compared to the capture antibody. Goat species antibody, used as a detector antibody, did not displace the same-species capture antibody. ELISA analysis showed detection of *Escherichia coli* O157:H7 cells at 1.0 x 10^4 CFU/ml using HSA-PG and goat antibody raised against *Escherichia coli* O157:H7; unlabeled antibody was used for capture while HRP labeled antibody was used for detection. Studies were performed on an automated fiber optic biosensor, RAPTOR, which was used for the rapid detection of pathogens.

Biosensor assays showed detection of *E. coli* O157:H7 at 1.0 x 10^3 CFU/ml in PBS and 1.0 x 10^5 CFU/ml in homogenized ground beef supernatant. Capture efficiency of the HSA-PG capture matrix was studied using the biosensor and GFP-*E. coli* O157:H7. The amount of cells captured was less than one percent of the sample concentration. This limit of detection and capture efficiency was comparable to the streptavidin-biotin capture matrix.

INTRODUCTION

Objective

Fluorescent immunoassays have been growing in popularity for use in the field of pathogen detection. In 1984, Hirschfeld patented the use of evanescent wave and optical fiber in an immunoassay format to detect fluorescent labeled analytes (15). Since this invention, optical fiber and fluorescent immunoassay have been developed for use in biosensor technology to rapidly detect pathogens in environmental samples (6, 19, 23). Biosensors detect targets that have been captured by a matrix of capture molecules attached to a solid surface such as an optical fiber or waveguide. However, antibody based biosensor assays are plagued by poor capture efficiency and low sensitivity (36). The goal of this research was to orient the capture antibody to enhance capture efficiency of a target bacterium. This increase in capture efficiency may improve assay sensitivity so that fewer bacterial cells are required for positive detection by the biosensor. This improved detection would benefit the public directly by promoting advances in food safety inspections and homeland security efforts. In order to investigate the hypothesis that orientation of antibodies would improve detection sensitivity, a novel capture matrix that presented antibodies in a uniform formation on a solid surface was developed and then examined to assess improvements made to capture efficiency or assay sensitivity.

Biosensor Assay

A sandwich biosensor assay consists of three phases as shown in Figure 1. The purpose of the Capture Phase is to immobilize antibodies which are specifically able to capture the target antigen. The Sample Phase is the introduction of liquid containing whole bacterial cells or small toxins. The sample may come from a variety of liquids such as homogenized ground meat supernatant, environmental water or phosphate buffered saline. The purpose of the Reporter Phase is to detect captured antigens by using a fluorescently labeled detector antibody specific for the target. The fluorescently labeled antibody is excited by a 635 nm laser focused through the core of the waveguide. The evanescent wave produced by the laser penetrates the surface of the waveguide to excite fluorophores within 100-1000 nm of the waveguide surface (11, 23). Emissions from the fluorophore are recoupled into the optical fiber and converted to picoamperes (pA) by a photodiode. Ultimately, the biosensor is a dedicated fluorometer that is able to collect and quantitate emitted wavelengths above 650 nm. Any of these phases can be modified in order to produce a more efficient and sensitive biosensor assay.

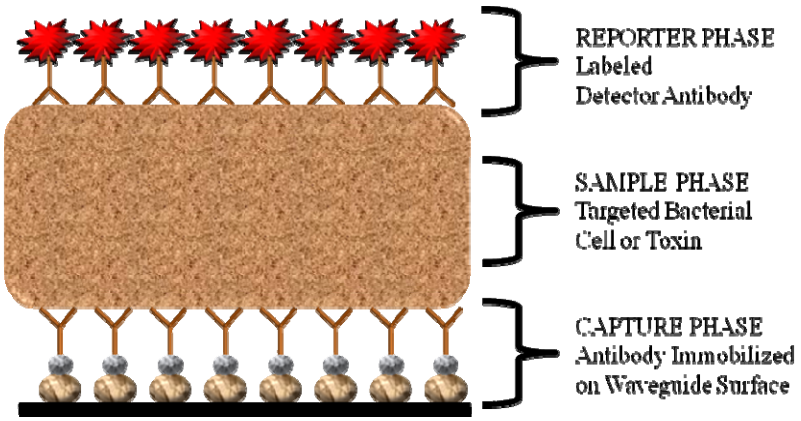

FIGURE 1. Biosensor Phases

Streptavidin-Biotin

Currently, biosensor capture surfaces are coated with a large homo-tetrameric protein isolated from the bacterium *Streptomyces avidinii* known as streptavidin (39). Streptavidin (60kDa) has an extremely high binding affinity (Ka = 2.5 $x10^{13}$) for the much smaller vitamin H (244 Da), more commonly called biotin (13). Streptavidin-biotin conjugation is widely used in microbiology and immunology due to this strong non-covalent interaction. Streptavidin has four subunits and each subunit can bind one biotin molecule. In solution, one streptavidin molecule can bind up to four biotin molecules simultaneously and with equivalent affinity (22). This strong binding ability has been utilized in a variety of assays, e.g., biotinylation of nucleic acids, amino acids and antibodies. The biotinylation enables the capture of targets by indirectly attaching them to a streptavidin coated surface. Biotinylated antibodies, anchored via streptavidin to fiber optic waveguides, have been reported in a number of recent biosensor manuscripts (6, 19, 36).

Random Antibody Orientation

Biotin can be attached to the carbohydrate moiety found on the crystallizable fragment (Fc) region, or to the primary amines ($-NH_2$) located on the numerous lysine residues found on the Fc, and antigen binding fragment (Fab) regions of an immunoglobulin G (IgG) molecule (16, 31). Hnatowich's method uses succinimidyl-6-(biotinamido) hexanoate (NHS-LC-Biotin) to biotinylate lysine residues on an IgG molecule (6). This labeling method results in a random orientation of the antibody, tilted at various angles on the waveguide surface, with paratopes that are not aligned for antibody-antigen interaction (31). As depicted in Figure 2, the antibodies are not oriented

efficiently on the waveguide for antigen capture. If the antibody is angled slightly, or laid on its side the antigen binding site is not likely to come into contact with the antigen, which results in missed capture opportunities. These missed opportunities may lead to poor bacterial capture efficiency by the capture matrix.

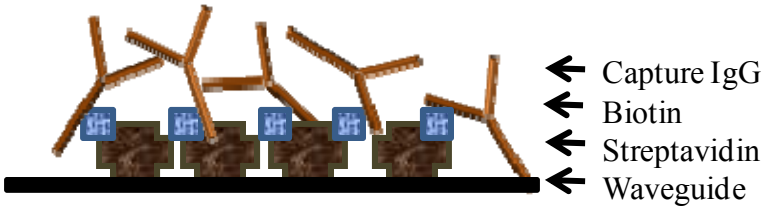

FIGURE 2. Orientation of Biotinylated Antibody on a Streptavidin Coated Waveguide

Human Serum Albumin

Working with human serum albumin (HSA) has many advantages beyond its common usage as a blocking agent in ELISA protocols (5). HSA (66 kDa) is an inexpensive transporter protein found abundantly in human plasma (5 g/ 100 ml). The ability of HSA to transport molecules to target organs has been exploited to deliver therapeutic drugs *in vivo* (38). Like many species of albumin, the structure of HSA is a single asymmetrical polypeptide contained in three, almost identical, homologous domains resultant from gene multiplication (8, 38). This simple albumin structure allows for high affinity and rapid binding to ligands, such as the albumin binding domain of streptococcal PG (29). The efficient coating of polystyrene surfaces by HSA removes the need for any additional blocking step, which allows the assay to be performed quickly (18).

Streptococcal Protein G

Lancefield group C and G streptococcal strains produce transmembrane bound Protein G (PG) to evade host immune responses. Membrane-bound PG binds to the Fc domain of an opsonizing antibody i*n vivo*, which prevents C1q, a subcomponent of the complement system, from recognizing the antibody and initiating the classical pathway (27). PG is a highly versatile protein; however, almost all commercially available PG is in a recombinant form. This recombinant form lacks the albumin binding domain located on the amino terminus of PG (17, 20, 29, 37). The albumin binding domain, if left intact, binds to serum albumin, making the protein inefficient at extracting and purifying antibodies from blood samples. The albumin binding domain of PG has been used to anchor antibody fragments to HSA coated polystyrene ELISA wells (18). Native PG, containing the albumin binding domain, can be used as an anchor to polystyrene surfaces that have been non-covalently coated with HSA, such as a fiber optic waveguide or ELISA wells. PG has a high amount of secondary structure and contains a hydrophobic core, which makes it a very heat-stable protein (7). The robust nature of PG contributes greatly to its appeal for use in biosensor assays.

In addition to the albumin binding domain, PG (65 kDa) has three identical IgG binding domains near the carboxyl terminus, which is structurally opposite from the albumin binding domain (14, 17, 20, 28, 30, 37). Only one of the three IgG binding domains, the most distal, has shown the ability to bind the carboxyl terminus of the heavy chain of intact IgG, or to the Fab region of fragmented IgG. This binding occurs without large conformational changes in the structure of either participant (7). PG has a high binding affinity (Ka = 5-10 x 10^{10}) for the heavy chain of the Fc domain of IgG

belonging to several different species, including goat, rabbit and human. The affinity of the PG Fc binding domain is minimal for mouse IgG (1, 4), and completely absent for chicken IgG (1, 14). This species specificity is due to the relatively conserved nature of the four gamma (γ) chains of the IgG molecule (14). Table 2 shows the relative affinities of several species of IgG.

Species of Polyclonal Immunoglobulin	Amount (ng) of Ig Required to Give a 50% Inhibition In Competitive ELISA
	Protein G
Rabbit	151
Goat	217
Human	556
Mouse	1020
Chicken	-

– Indicates Species Not Reactive with Fc Binding Domain on PG

TABLE 1. Species Specificity of the Fc Binding Domain on PG (14)

The PG-IgG Complex

The binding of the PG IgG-binding domain to the carboxyl terminus of the heavy chain of IgG involves a large amount of surface area on both molecules, creating a binding affinity comparable to antigen-antibody complexes (Ka = 5-10 x 10^{11}) (7). In addition to multiple hydrogen bonds and van der Waals attractions, the bound complex remains intact in solution due to a hydrophobic area, created by the interaction of side chains of charged residues. This conformational binding was observed while the molecule was in crystal form, as well as in solution, indicating that liquid would not denature the PG-IgG complex (7).

Antibody Orientation by HSA-PG

The uniform orientation of an antibody on a solid surface increases its activity by promoting interactions between antigen, and antigen binding sites, as compared to random antibody orientation (40). Streptococcal PG binds specifically to the carboxyl terminus of the Fc region of an IgG molecule, which causes the Fab region to face outward (21, 25). This uniform orientation of immobilized IgG on HSA-PG can be attached to a solid surface for use in a biosensor assay or ELISA, and may lead to increased capture efficiency and sensitivity. PG binding to the Fc domain of an IgG molecule dictates the orientation of the antibody when attached to an albumin protein coated surface (7).

FIGURE 3. Orientation of Antibody on a HSA-PG Coated Waveguide Surface

Capture Efficiency

Recently, the capture efficiency of evanescent waved based biosensor assays using a streptavidin-biotin-IgG capture matrix has been under review (36). *Escherichia coli* O157:H7 expressing green fluorescent protein was used to quantitate target cell capture on planar and cylindrical waveguides using an automated and manual biosensor. Capture efficiencies were inversely related to the concentration of sample introduced into the matrix (36). One possible explanation for the poor capture efficiency was the random

orientation of capture antibody on the waveguide surface. Random antibody orientation reduces antibody activity when the antibody is attached to a sold surface (24, 40). Capture efficiency may be improved by replacing the streptavidin-biotin-IgG capture matrix with an HSA-PG-IgG capture matrix, which uniformly orients the capture antibody to increase interactions with the targeted antigen.

Hypothesis

A novel capture matrix consisting of human serum albumin, streptococcal Protein G and capture antibody (HSA-PG-IgG) would uniformly orient capture antibodies on a solid surface, increasing capture efficiency of bacteria. More efficient bacterial capture would result in a higher signal-to-noise ratio, enhancing sensitivity of the assay.

MATERIALS AND METHODS

Bacterial Strains

Escherichia coli O157:H7 was provided by the Massachusetts Department of Public Health State Laboratory Institute (Jamaica Plain, MA), and was used as the target antigen in all specificity and sensitivity studies. This environmental strain was recovered from taco meat distributed at a county fair, which resulted in an outbreak of food poisoning in Massachusetts. The strain was received by our laboratory in December 1998 and was stored at -80ºC in sterile glycerol. A green fluorescent protein expressing stock of *Escherichia coli* O157:H7 ATCC#35150 (GFP-*E. coli* O157:H7) was used in all capture efficiency studies. The 5.4 kb GFP-encoded plasmid encoded ampicillin resistance and was regulated by an arabinose promoter which was activated by specialized media described in the Media and Culture Conditions section (36).

Escherichia coli K-12 was purchased from the American Type Culture Collection (ATCC#23590). *E. coli* K-12 was used as a negative control in all specificity and sensitivity studies.

Buffers

Sodium phosphate-buffered saline, 0.1 M and pH 7.4, (PBS) contained 3.2 g NaH_2PO_4, 20.6 g Na_2HPO_4 and 8 g NaCl per liter of filter (0.22 μm) sterilized water (Millipore; Billerica, MA). PBS with 0.05% Tween 20 (PBST) was used to remove any unbound reagents during rinsing steps.

Media and Culture Conditions

Stock Cultures

Cultures of *E. coli* O157:H7 and *E. coli* K-12 were grown on tryptic soy agar (TSA) for 18 hours at 37ºC, then stored at 4ºC for up to two weeks before being used to prepare sample cultures. GFP expressing *E. coli* O157:H7 (GFP-*E. coli* O157:H7) was maintained on Luria Bertani (LB) media containing 100 µg/ml ampicillin (AMP) and 5 mg/ml arabinose (ARA) (LB+AMP+ARA). After 18 hours of growth at 37ºC the LB+AMP+ARA plates were inverted and stored at 4ºC for up to two weeks before being used to prepare sample broth cultures. All media was purchased from Becton Dickinson (Franklin Lakes, NJ) and was reconstituted and sterilized according to the manufacturer's directions.

Sample Cultures

A single colony from a TSA plate was used to prepare a broth culture of *E. coli* O157:H7 or *E. coli* K-12 in tryptic soy broth (TSB). A single colony from an LB+AMP+ARA plate was used to prepare a broth culture of GFP- *E. coli* O157:H7 in LB+AMP+ARA broth. Broths were purchased from Becton Dickinson (Franklin Lakes, NJ) and were reconstituted and sterilized according to the manufacturer's directions. A broth culture used in an experiment was grown in 10 ml of appropriate broth in a 50 ml conical tube for 18 hours at 37ºC with shaking at 200 r.p.m. The culture was then diluted (1:100) in fresh broth and returned to the shaking incubator for 4-6 hours until an optical density at 600 nm (OD_{600}) of 0.6-1.0 was reached. Optical densities were measured using a DU®-64 spectrophotometer (Beckman, Fullerton, CA). The sample culture was serially diluted in PBS for use in an assay. The bacterial dilution was maintained at 24ºC in PBS

for one hour, and then it was vortexed for twenty seconds using a Fisher Vortex Genie 2 (Fisher Scientific; Suwanee, GA) to homogenize the cell culture. Once a homogeneous solution was reached, the bacterial dilution was added to the assay.

The cell concentration for each sample culture was determined using viable count. One hundred microliters of GFP-*E. coli* O157:H7 was plated onto an LB+AMP+ARA plate, then incubated for 18 hours at 37ºC to allow growth of colonies. *E. coli* O157:H7 and K-12 were similarly plated onto TSA to obtain viable counts. Sorbitol-MacConkey agar (SMAC) (Remel; Lenexa, KS) was used to recover and presumptively differentiate between *E. coli* O157:H7 and K-12 colonies. *E. coli* O157:H7 was unable to ferment sorbitol and produced colorless colonies on the SMAC plate. Alternatively, *E. coli* K-12 was able to ferment sorbitol and produced pink or purple colonies on the SMAC plate.

Capture Matrix Proteins

Albumins

Ovalbumin (OVA) and human serum albumin (HSA) fraction V (96-99% purity by agarose gel electrophoresis) was purchased from Sigma-Aldrich (St. Louis, MO). Bovine serum albumin (BSA) was purchased from Fisher Scientific (Suwanee, GA). Lyophilized albumin crystals were rehydrated in 50% (v/v) glycerol, and 40 µl aliquots were stored at -20ºC in microfuge tubes. Working dilutions were prepared in PBS.

Protein G and Streptavidin

Native Protein G (PG) from S*treptococcus* species was purchased from Calbiochem (San Diego, CA). Streptavidin and PG lacking the albumin binding domain (recombinant PG) were purchased from Sigma-Aldrich. These lyophilized proteins were

rehydrated to 1.0 mg/ml in PBS, and 40 µl aliquots were stored at -20ºC in microfuge tubes. Working dilutions were prepared in PBS.

Antibodies

Lyophilized goat polyclonal antibody raised against *E. coli* O157:H7 and horse radish peroxidase labeled (HRP) labeled, biotin labeled or unlabeled (KPL; Gaithersburg, MD), was rehydrated in 50% (v/v) glycerol to 1.0 mg/ml. Mouse monoclonal antibodies, isotype IgG3, raised against *E. coli* O157:H7 were purchased from Abcam (Cambridge, MA), Biodesign International (Saco, ME), U.S. Biological (Swampscott, MA) and Fitzgerald (Concord, MA), and were diluted to 0.1 mg/ml in 50% (v/v) glycerol. Lyophilized mouse monoclonal antibody raised against rabbit or goat immunoglobulin; and HRP labeled, goat polyclonal antibody raised against mouse immunoglobulin; and rabbit polyclonal antibody raised against goat immunoglobulin; and HRP labeled or unlabeled rabbit (Jackson Immuno Research; West Grove, PA), was rehydrated in 50% (v/v) glycerol to 1.0 mg/ml. Lyophilized rabbit polyclonal antibody raised against PG (Abcam; Cambridge, MA), and lyophilized chicken polyclonal antibody raised against mouse immunoglobulin and HRP labeled (U.S. Biological; Swampscott, MA) was rehydrated in 50% (v/v) glycerol to 1.0 mg/ml. To avoid protein degradation each antibody was divided into 40 µl aliquots which were stored at -20ºC. Frozen antibody aliquots were used one time and never refrozen. Chicken polyclonal antibody raised against mouse immunoglobulin and HRP labeled (Aves Labs; Tigard, OR) was stored at 4ºC.

Antibody Labeling

Cy5 Antibody Labeling Column

A column, used to separate unbound dye from labeled antibody, was prepared twenty four hours before labeling. In a 50 ml conical tube 1.4 g Bio-Gel P-10 fine (Bio-Rad, Hercules, CA) was saturated with 20 ml PBS containing 0.02% (v/v) NaN_3 (PBS-NaN_3). The gel was allowed to hydrate at 24ºC for 4 hours. A 20 ml Econo Pac column (Bio-Rad) was secured to a column stand and the end was snapped off. The Bio-Gel mix was thinned by the addition of 40 ml PBS-NaN_3. After inverting the conical tube the slurry was transferred by pipette into the purification column. The gel was allowed to settle and excess buffer was drained. Once the gel settled, a frit was applied on top of the gel bed. A thin layer of PBS-NaN_3 was applied to keep the frit moist. The column was then stored at 4ºC for twenty-four hours.

Cy5 Antibody Labeling Procedure

Antibody labeling was performed using a cyanine 5 dye (Cy5) labeling kit (Fluorolink™Cy5™Reactive Dye 5-pack, Amersham Life Sciences; Arlington Heights, IL). Lyophilized goat polyclonal antibody raised against *E. coli* O157:H7 was rehydrated in sodium carbonate buffer [0.1 M, pH 9.3] to 1.0 mg/ml. The antibody solution was transferred to a tube containing Cy5 reactive dye. The tube was capped and protected from light while it was incubated for one hour at 24ºC. The contents of the reaction tube were transferred by pipette onto the column frit. The contents were flushed from the frit by the addition of PBS, and clear liquid was collected as waste. The first of two blue bands observed moving through column was collected in an amber microfuge tube as labeled antibody. The second blue band consisted of unbound Cy5, and was discarded as

waste. The purification column was rinsed for 30 minutes with PBS-NaN_3, then secured and stored at 4ºC for reuse within three months. The concentrations of antibody and Cy5 dye in the labeled product were determined by measuring the absorbance at 280 nm (A_{280}) and 650 nm (A_{650}), respectively; and applying the Beer-Lambert Law, which explains the linear relationship between absorbance and concentration of the absorbing substance. These concentrations were also used to determine the protein to dye ratio, which was the amount of dye particles conjugated to each protein molecule. Absorbencies were measured using a DU®-64 spectrophotometer (Beckman; Fullerton, CA).

$$\text{Concentration of Antibody (M)} = \frac{(A_{280} - (0.05 \times A_{650}))}{1 \text{ cm} \times 170{,}000 \text{ M}^{-1} \text{ cm}^{-1}}$$

$$\text{Concentration of Cy5 (M)} = \frac{(A_{650})}{1 \text{ cm} \times 250{,}000 \text{ M}^{-1} \text{ cm}^{-1}}$$

$$\text{Dye to Protein Ratio} = \frac{[\text{Antibody (M)}]}{[\text{Cy5 (M)}]}$$

TABLE 2. Equations for Cy5 Labeling of Antibody

DyLight™649 Antibody Labeling Procedure

Antibody labeling was performed using a DyLight™ antibody labeling kit (Pierce Biotechnology; Rockford, IL). The labeling buffer [50 mM sodium borate pH 8.8] was prepared by combining 925 µl of PBS with 75µl of sodium borate buffer [67 mM]. Five hundred microliters of labeling buffer was added to 1.0 mg of lyophilized goat polyclonal

antibody raised against *E. coli* O157:H7 to obtain a concentration of 2.0 mg/ml. The rehydrated antibody was transferred to a vial containing DyLight™649 reactive dye. The vial was gently inverted for ten seconds, and then centrifuged for thirty seconds to concentrate the protein at the bottom of the vial. The tube was protected from light and incubated for one hour at 24ºC. Two purification spin columns were placed inside two collection tubes and four hundred microliters of purification resin was added to each of the spin columns. The spin columns were centrifuged for 45 seconds at 1,000 x g to remove excess storage buffer, then the collection tubes were replaced by new tubes to collect the purified protein. Labeled antibody was evenly divided into the two spin columns, and then the columns were centrifuged for 45 seconds at 1,000 x g to separate unbound fluorophore from labeled antibody. The contents of the two collection vials were combined, and the concentrations of antibody and dye in the labeled product were determined by measuring the absorbance at 280 nm (A_{280}) and 654 nm (A_{654}), respectively. The Beer-Lambert Law was applied to these values. These concentrations were used to determine the protein to dye ratio, which was the amount of dye particles conjugated to each protein molecule. Absorbencies were measured using a DU®-64 spectrophotometer (Beckman; Fullerton, CA).

$$\text{Concentration of Antibody} = \frac{(A_{280} - (0.0371 \times A_{654})) \times \text{Dilution Factor}}{210{,}000\ M^{-1}\ cm^{-1}}$$

$$\text{Dye to Protein Ratio} = \frac{(A_{654}) \times \text{Dilution Factor}}{[\text{Antibody}] \times 250{,}000\ M^{-1}\ cm^{-1}}$$

TABLE 3. Equations for DyLight™649 Labeling of Antibody

ELISAs

PG Fc Binding Domain Specificity Assays

One hundred microliters of HSA [0.5 or 1.0 μg/ml] was added to wells of a 96 well Nunc Immuno plate and allowed to incubate for 18 hours at 4ºC to determine the functionality and specificity of the Fc binding domain of PG. After incubation, the plate was washed three times with PBST using an ELx50 Auto Strip Washer (Bio-Tek Instruments, Inc.; Winooski, VT). One hundred microliters of native PG [0 - 2.5 μg/ml] was added to albumin coated wells and allowed to incubate for 60 minutes at 24ºC. The plate was then washed three times with PBST. For competitive ELISAs, mouse monoclonal or goat polyclonal antibodies raised against rabbit immunoglobulin and labeled with HRP was mixed in equal concentrations [0 - 1.0 μg/ml] in a microfuge tube, with unlabeled mouse monoclonal or goat polyclonal antibody raised against *E. coli* O157:H7. One hundred microliters of the antibody combination was transferred into the ELISA well, and was incubated for 30 minutes at 24ºC. The plate was then washed three times with PBST. For indirect ELISAs, 100 μl of primary antibody [1.0 μg/ml], rabbit polyclonal antibody raised against goat immunoglobulin or goat polyclonal antibody raised against *E. coli* O157:H7, was added to the wells, and was incubated for 30 minutes at 24ºC. The plate was then washed three times with PBST. One hundred microliters of mouse monoclonal antibody raised against rabbit or goat immunoglobulin and HRP labeled [0.1 or 0.5 μg/ml], was added to the ELISA wells, and was incubated for 30 minutes at 24ºC. The plate was then washed three times with PBST. A QuantaBlu™ Fluorogenic Peroxidase Substrate Kit (Pierce; Rockford, IL) was used to activate the peroxidase activity of antibodies labeled with HRP. Signals were detected and quantified

using a Spectra Max Gemini XS Microplate Fluorometer (Molecular Devices; Sunnyvale, CA) with excitation, emission, and cutoff wavelengths set at 340nm, 470nm and 455, respectively.

PG Albumin Binding Domain Functionality and Specificity Assays

One hundred microliters of HSA, ovalbumin (OVA) or bovine serum albumin (BSA) [0.5, 1 or 5 μg/ml] was added to a 96 well Nunc Immuno plate and allowed to incubate for 18 hours at 4ºC to determine the functionality and specificity of the albumin binding domain of PG. After incubation, the plate was washed three times with PBST using an ELx50 Auto Strip Washer (Bio-Tek Instruments, Inc.; Winooski, VT). One hundred microliters of native or recombinant PG [0-5 μg/ml] was added to the albumin coated wells, and allowed to incubate for 8 or 60 minutes at 24ºC. The plate was then washed three times with PBST. One hundred microliters of primary antibody [1.0 μg/ml], rabbit polyclonal antibody raised against PG or goat immunoglobulin was added to wells, and allowed to incubate for 30 minutes at 24ºC. The plate was then washed three times with PBST. One hundred microliters of mouse monoclonal antibody raised against rabbit immunoglobulin and HRP labeled [0.1 or 0.5 μg/ml] was added to wells, and was incubated for 30 minutes at 24ºC. The plate was then washed three times with PBST, and then analyzed for fluorescence using a QuantaBlu™ Fluorogenic Peroxidase Substrate Kit (Pierce; Rockford, IL) to activate the peroxidase activity of antibodies labeled with HRP. Signals were detected and quantified using a Spectra Max Gemini XS Microplate Fluorometer (Molecular Devices; Sunnyvale, CA) with excitation, emission, and cutoff wavelengths set at 340nm, 470nm and 455, respectively.

Direct Assays for Detection of E. coli O157:H7

One hundred microliters of HSA [0 - 80 μg/ml] was added to a 96 well Nunc Immuno Plate (Fisher Scientific; Suwanee, GA), and was incubated for 18 hours at 4ºC to capture *E. coli* O157:H7 for detection by ELISA. After incubation, the plate was washed three times with PBST using an ELx50 Auto Strip Washer (Bio-Tek Instruments, Inc.; Winooski, VT). Native or recombinant PG [0-10 μg/ml] was added to HSA coated wells, and was incubated for 30 minutes at 24ºC. The plate was then washed three times with PBST. Capture antibody [0-5.0 μg/ml], goat polyclonal antibody raised against *E. coli* O157:H7, was added to wells, and was incubated for 30 minutes at 24ºC. The plate was then washed three times with PBST. One hundred microliters of *E. coli* O157:H7 or K-12 was added to wells, and was incubated for 30 minutes at 24ºC; and then the plate was washed three times with PBST. One hundred microliters of mouse monoclonal or goat polyclonal antibody, raised against *E. coli* O157:H7 and HRP labeled [0.1 μg/ml], was added to wells, and was incubated for 30 minutes at 24ºC. The plate was then washed three times with PBST, and analyzed for fluorescence using a QuantaBlu™ Fluorogenic Peroxidase Substrate Kit (Pierce; Rockford, IL) to activate the peroxidase activity of antibodies labeled with HRP. Signals were detected and quantified using a Spectra Max Gemini XS Microplate Fluorometer (Molecular Devices; Sunnyvale, CA) with excitation, emission, and cutoff wavelengths set at 340nm, 470nm and 455, respectively.

Statistical Analysis

A one-way ANOVA with Dunnett's post test was performed using GraphPad InStat 3.00 (San Diego, CA) for all ELISAs. Paired data, in normal Gaussian distribution, was analyzed using a t test with a two tailed P value. Statistically significant P values (<

0.05) were noted on the graphs to aid in the analysis of the data. Raw data was analyzed using Microsoft Excel.

RAPTOR ASSAYS

Coupon Preparation

Four polystyrene waveguides, of approximately 38 mm in length, were sonicated in isopropanol for thirty seconds, and then rinsed in 250 ml of water that was filter (0.22 μm), and ultraviolet light sterilized, using a Milli-Q® Synthesis System (Millipore; Billerica, MA). The waveguides were allowed to dry for 30 minutes with optical heads facing down. Then the distal tip of each waveguide was coated with matte black ink, to provide a light dump for the 635nm laser beam, and was dried for two hours at 24ºC. One waveguide was glued into each of the four channels of the RAPTOR (Research International, Monroe, WA) coupon. The optical glue (Norland Products, Inc; Cranbury, NJ) was dried for 30 minutes using a long-wavelength ultraviolet lamp at 24ºC. Once the glue dried, the coupon was sealed in a small storage bag and stored at 24ºC for one to thirty days.

Waveguide Preparation

Twenty-four hours before a RAPTOR assay was performed 100 μl of HSA [100 μg/ml] was added to two of the waveguides in a coupon, while the other two waveguides in the coupon were coated with 100 μl of streptavidin [100 μg/ml]. The treated waveguides were incubated for 18 hours at 4ºC, and then any excess protein was removed from the coupon by rinsing each waveguide three times with PBST. One hundred microliters of PG [50 μg/ml] was added to the HSA treated waveguides and allowed to incubate for 15 minutes at 24ºC. Any unbound PG was aspirated from the waveguides,

and fresh PG was added for a second 15 minute incubation. HSA-PG and streptavidin coated waveguides were rinsed three times with PBST. Goat polyclonal antibody raised against *E. coli* O157:H7 [50 µg/ml] was added to the HSA-PG treated waveguides; and goat polyclonal antibody raised against *E. coli* O157:H7 and biotin labeled [50 µg/ml] was added to streptavidin treated waveguides. Antibody solutions were incubated for 30 minutes at 24ºC. Any unbound antibody was aspirated from the waveguides, and fresh antibody was added for a second 30 minute incubation. Each waveguide was rinsed three times with PBST. Once the waveguides in the coupon were treated with the appropriate capture matrix, the back side of the coupon was sealed with tape to prevent fluid leakage, and to maintain vacuum pressure inside the individual channels. To operate the biosensor, each RAPTOR assay was an automated function defined by a unique recipe, which was encoded by a certain number ranging from 0 to 63. The biosensor determined which recipe to follow based on a recipe card that was attached to the coupon, and marked with the appropriate recipe number. To avoid channel-related bias in the data, the position of the differently treated waveguides was alternated for each assay replicate.

RAPTOR Assay Procedure

The RAPTOR biosensor was assembled by connecting a piece of tubing to the buffer inlet and placing the other end in a container of PBST. Detector antibody, 1.0 ml, was placed in each of four reagent vials, and then tubing was used to connect the reagent vials with the reagent ports on the biosensor. A previously assembled coupon was placed securely into the biosensor, and the assay protocol was then commenced. A series of four blank samples consisting of 2.0 ml of PBS, injected into the sample port, were sequentially assayed to determine the background signal. The thirty-two minute assay

consisted of a 500 µl sample pulsed twelve times (40 µl of sample per pulse) over each of the four waveguides, with a two minute incubation period between pulses. The waveguides were then rinsed for 30 seconds with PBST. Two hundred microliters of detector antibody was pumped into each of the four waveguide channels and allowed to incubate for two minutes. After the incubation, the reagent pump was reversed to withdraw the detector antibody back into the reagent tubes. The waveguides were then rinsed twice for 30 seconds with PBST.

Detection of the target was measured by fluorescence of the immune bound detector antibody, goat polyclonal antibody raised against *E. coli* O157:H7 and Cy5 or DyLight™649 labeled [5.0 µg/ml], for direct sandwich assays. After the baselines were determined, samples containing *E. coli* O157:H7 were interrogated by the capture matrix. Fluorescence emissions, within 100 - 1000 nm of the waveguide surface, were measured in picoamperes (pA) by a photodiode able to collect and quantitate emitted wavelengths above 650 nm.

Blank samples were immediately followed by bacterial samples consisting of *E. coli* O157:H7 [1 x 10^{2-7} CFU/ml], beginning with the lowest concentration, for limit of detection assays. Typically, three to four bacterial sample concentrations were tested per RAPTOR coupon. For capture efficiency assays, blank samples were immediately followed by one bacterial sample consisting of GFP-*E. coli* O157:H7 [1 x 10^{6-8} CFU/ml]. Direct counts, using a Cellometer™ slide (Nexcelom Bioscience; Lawrence, MA), were used to determine sample concentrations (cells/ml) before the assays were performed. For data analysis, viable counts were performed on TSA or LB+AMP+ARA respectively, to determine sample concentrations (CFU/ml) retroactively. All RAPTOR data was

analyzed by Microsoft Excel. For capture efficiency experiments, assayed coupons were sealed in a plastic bag and stored at 4ºC for 24 to 72 hours until analyzed by fluorescent microscopy.

Determination of Capture Efficiencies

Cells captured on the waveguide were manually counted using a UIS2 LUCPlan FLM 20X long range objective mounted on an Olympus BX60 Epifluorescent microscope (Olympus America Inc.; Center Valley, PA). The optical head of each waveguide was carefully removed using a sterile razor blade. The waveguide was then secured to a clean glass slide using craft glue. After the glue dried (~2 minutes) photographs were taken using a SPOT Flex™ color CCD camera (Diagnostic Instruments Inc.;Sterling Heights, MI) and imaged using Adobe® Photoshop® Basic (Adobe Systems Inc; San Jose, CA). Cells were counted and averaged using three images per waveguide. Each viewable field represented 1 mm of waveguide length. Only 46 out of 360 degrees of the waveguide surface were viewable, so the average number of cells counted was multiplied by a correction factor (7.8 = 360º / 46º) to achieve the number of cells per mm of each waveguide. As depicted in Table 4, the number of cells counted per mm was multiplied by the length of the waveguide, 38mm, to produce the number of cells present on the surface of the entire waveguide.

= (Number of Cells on Three WGs / 3) * (360º/46º Viewable Angle) * Length of WG
= Average Number of Cells per mm * 7.8 * 38 mm
= Average Number of Cells per Waveguide

$$\text{Capture Efficiency} = \frac{\text{Average Number of Cells per Waveguide}}{\text{Sample Concentration (CFU/ml)}}$$

TABLE 4. Capture Efficiency Calculations

Detection of E. coli O157:H7 in Food Samples

Ten grams of spinach or ground beef (20% fat) obtained from local grocers was placed in a Whirl-Pak® filter bag (Nasco; Fort Atkinson, WI) and inoculated with 1.0 ml of *E. coli* O157:H7 in PBS, and stored for 18 hours at 4°C. Fifty milliliters of buffered peptone water (BPW) was added to the filter bag, and then the samples were homogenized for thirty seconds using a Pulsifier (Microbiology International; Frederick, MD). The supernatant was removed and transferred to a 50 ml conical tube. Serial dilutions of the supernatant were prepared in BPW, and were used in the assay. The homogenized samples were assayed as described in the RAPTOR Assay Procedure section.

Data Analysis

Signal above the limit of detection (SALOD) values were calculated for each RAPTOR assay. The SALOD values were determined based on a method used to normalize the waveguides within each coupon. Each coupon contained four waveguides, and was considered an independent assay. Baselines were performed as described in the RAPTOR Assay Procedure section. Table 5 represents typical baseline values from a

RAPTOR assay. The values in bold were the lowest value for each baseline. Typically, the same waveguide produced all four of the lowest baseline values for each assay.

	Waveguide 1	Waveguide 2	Waveguide 3	Waveguide 4
Baseline 1	672.7	584.7	576.1	**402.8**
Baseline 2	703.4	594.4	617.9	**433.6**
Baseline 3	731.0	612.9	641.7	**465.5**
Baseline 4	763.8	623.1	675.8	**489.6**

TABLE 5. Baseline Values

The four waveguide values were divided by the bolded value to achieve a normalization coefficient, for each baseline. Table 8 shows the normalization coefficients for the baseline values from Table 5.

	Waveguide 1	Waveguide 2	Waveguide 3	Waveguide 4
Baseline 1	1.7	1.5	1.4	1.0
Baseline 2	1.6	1.4	1.4	1.0
Baseline 3	1.6	1.3	1.4	1.0
Baseline 4	1.6	1.3	1.4	1.0

TABLE 6. Normalization Coefficients

The normalization coefficients, from Table 6, were used to normalize the baseline values from Table 5. For each waveguide, the baseline values from Table 5 were divided by the normalization coefficient for Baseline 4 in Table 6. Typically, the normalization coefficients did not vary between the third and fourth baseline. Table 7 shows the normalized baseline values.

	Waveguide 1	Waveguide 2	Waveguide 3	Waveguide 4
Baseline 1	431.2	459.4	417.4	402.8
Baseline 2	450.9	467.0	447.7	433.6
Baseline 3	468.6	481.6	464.9	465.5
Baseline 4	489.6	489.6	489.6	489.6

TABLE 7. Normalized Baseline Values

The normalized baselines, in Table 7, were evaluated for variability. For each waveguide, the four normalized baseline values were averaged and the standard deviation was calculated. A coefficient of variation (CoV) was determined by dividing the average normalized baseline value by the standard deviation. The CoV was then multiplied by 100 to achieve a percentage. Data from any waveguide with a CoV percentage greater than ten was not used for data analysis or graph construction. Table 8 shows that all of the waveguides had baseline values with minimal variability.

	Waveguide 1	Waveguide 2	Waveguide 3	Waveguide 4
Average	460.1	474.4	454.9	447.9
STDEV	24.9	13.7	30.4	37.8
CoV (%)	5.4	2.9	6.7	8.4

TABLE 8. Normalized Baseline Variability

The limit of detection was determined to be the sum of the average normalized baseline plus three times the standard deviation, for each waveguide. Table 9 shows the level of detection for a typical RAPTOR assay.

	Waveguide 1	Waveguide 2	Waveguide 3	Waveguide 4
LOD	534.8	515.4	546.0	561.3

TABLE 9. Limit of Detection

Once the LOD was calculated, the bacterial samples were assayed as described in the RAPTOR Assay Procedure section. Table 10 shows the sample values for a typical RAPTOR assay used to detect a series of *E. coli* O157:H7 concentrations.

(CFU/ml)	Waveguide 1	Waveguide 2	Waveguide 3	Waveguide 4
1.4×10^2	796.0	637.5	721.2	519.8
1.4×10^3	860.1	671.9	765.6	546.0
1.4×10^4	1286.5	956.0	1050.0	782.6

TABLE 10. Bacterial Sample Values

The bacterial sample values were also normalized. For each waveguide, the values in Table 10 were divided by the normalization coefficients for Baseline 4 in Table 6. Table 11 shows the bacterial sample values after normalization.

(CFU/ml)	Waveguide 1	Waveguide 2	Waveguide 3	Waveguide 4
1.4×10^2	510.2	500.9	522.5	519.8
1.4×10^3	551.3	527.9	554.7	546.0
1.4×10^4	824.7	751.2	760.7	782.6

TABLE 11. Normalized Bacterial Sample Values

The level of detection value from Table 9 was subtracted from the bacterial sample value in Table 10 to determine if the normalized bacterial sample value was positive or negative for the detection of *E. coli* O157:H7, for each waveguide.

(CFU/ml)	Waveguide 1	Waveguide 2	Waveguide 3	Waveguide 4
1.4×10^2	-24.6	-14.5	-23.5	-41.5
1.4×10^3	16.5	12.5	8.7	-15.3
1.4×10^4	289.8	235.7	214.7	221.3

TABLE 12. Final Detection Values

Table 12 shows the finalized values for the detection of *E. coli* O157:H7 by the RAPTOR biosensor. A positive remainder was considered a positive detection of the target bacterium. A negative remainder indicated a negative detection of the target bacterium. For this example of a typical RAPTOR assay, the lowest concentration of *E. coli* O157:H7 detected was 1.4×10^3 CFU/ml for waveguides 1, 2 and 3; while waveguide 4 detected *E. coli* O157:H7 at 1.4×10^4 CFU/ml.

Statistical Analysis

A one-way ANOVA with Dunnett's post test was performed using GraphPad InStat 3.00 (San Diego, CA), for all RAPTOR assays. Paired data, in normal Gaussian distribution, was analyzed using a t test with a two tailed P value. Statistically significant P values (< 0.05) were noted on the graphs to aid in the analysis of the data. Raw data was analyzed using Microsoft Excel.

RESULTS AND ANALYSIS

Functional Albumin Binding Domain

Indirect ELISAs were performed as described in the Materials and Methods section to verify the presence and functionality of the albumin binding domain in native PG, and a lack of albumin binding by recombinant PG.

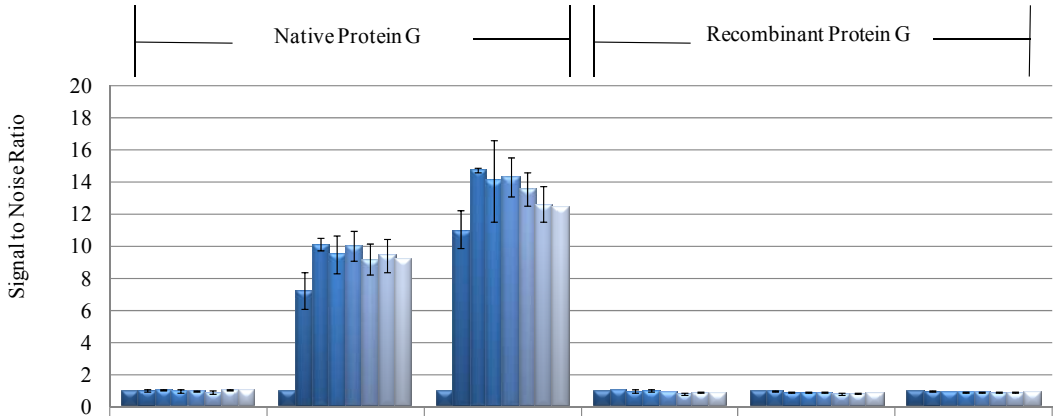

	0.0 µg/ml HSA	0.5 µg/ml HSA	1.0 µg/ml HSA	0.0 µg/ml HSA	0.5 µg/ml HSA	1.0 µg/ml HSA
PG 0.0 µg/mL	1.0	1.0	1.0	1.0	1.0	1.0
PG 0.25 µg/mL	1.0	7.2	11.1	1.1	1.0	1.0
PG 0.5 µg/mL	1.1	10.1	14.7	1.0	0.9	0.9
PG 1 µg/mL	1.0	9.5	14.1	1.0	0.9	1.0
PG 2.5 µg/mL	1.0	10.0	14.3	1.0	0.9	0.9
PG 5 µg/mL	0.9	9.2	13.6	0.8	0.8	0.9
PG 10 µg/mL	1.1	9.4	12.6	0.9	0.8	0.9
PG 20 µg/mL	1.1	9.3	12.5	0.9	0.9	1.0

FIGURE 4. Verification of a Functional Albumin Binding Domain in Native PG Using ELISA Analysis. Rabbit polyclonal antibody [1.0 µg/ml], raised against goat immunoglobulin, was used as the primary antibody; while mouse monoclonal antibody [0.1 µg/ml], raised against rabbit immunoglobulin, and HRP labeled, was used as the secondary antibody. HSA (shown on graph) was used to immobilize PG (shown on

graph) before antibodies were added to the assay. Each column, and coinciding standard deviation bar, was calculated from the average of six data points; which were collected from three independent assays.

A signal to noise ratio less than 2 was produced by all wells that contained recombinant PG (Figure 4). These low signals indicated the inability of recombinant PG to bind HSA. A signal to noise ratio greater than 2 was produced by all wells that contained native PG, which indicated that PG was bound to HSA. Native PG was implemented in all future assays for albumin binding.

Alternative Albumin Species

HSA was compared to other species of albumin to determine if it was the optimal species to immobilize PG in the capture matrix. Chicken ovalbumin (OVA) and bovine serum albumin (BSA) were tested as alternatives to HSA. Binding to PG, by OVA, BSA and HSA, was measured using indirect ELISAs as described in the Materials and Methods section.

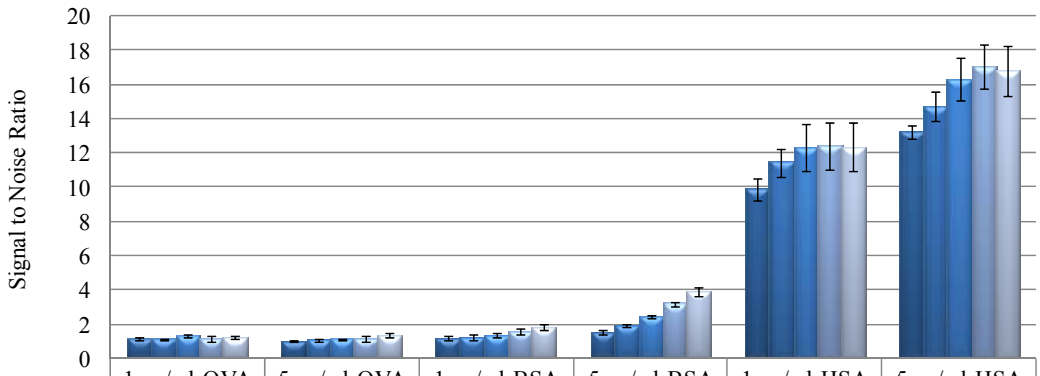

	1 µg/ml OVA	5 µg/ml OVA	1 µg/ml BSA	5 µg/ml BSA	1 µg/ml HSA	5 µg/ml HSA
0.25 µg/ml PG	1.1	1.0	1.2	1.5	9.9	13.2
0.5 µg/ml PG	1.1	1.1	1.2	1.9	11.4	14.7
1 µg/ml PG	1.3	1.2	1.3	2.5	12.3	16.3
2.5 µg/ml PG	1.2	1.2	1.6	3.2	12.4	17.1
5 µg/ml PG	1.2	1.3	1.9	3.9	12.4	16.8

FIGURE 5. Verification of Specificity of Different Albumin Species for PG Using ELISA Analysis. Rabbit polyclonal antibody [1.0 µg/ml], raised against PG, was used as the primary antibody; while mouse monoclonal antibody [0.5 µg/ml], raised against rabbit immunoglobulin, and HRP labeled, was used as the secondary antibody. OVA, BSA, or HSA (shown on graph) was used to immobilize PG (shown on graph) before antibodies were added to the assay. Each column, and coinciding standard deviation bar, was calculated from the average of six data points; which were collected from three independent assays.

A signal to noise ratio greater than 2 was produced only by wells that contained HSA at 1.0 and 5.0 µg/ml, and for BSA at 5.0 µg/ml (Figure 5). A signal to noise ratio less than 2 was produced by wells that contained OVA at 1.0 and 5.0 µg/ml, and for BSA at 1.0 µg/ml. The low signal to noise ratio produced from OVA indicated a lack of binding between PG and OVA. A high concentration of BSA was required to produce a signal to noise ratio greater than 2, when compared to HSA. These data indicated that

BSA bound PG, but only at high BSA concentrations. A minimal concentration of HSA produced high signal to noise ratio (> 8). The signal to noise ratio for the lowest concentration of HSA-PG (9.9) was nearly three times the signal to noise ratio for the highest concentration of BSA-PG (3.9). These data indicated that the albumin binding domain of PG had greater affinity for HSA. These results indicated that HSA was the optimal albumin species for use in the alternative capture matrix. HSA was implemented as the albumin used to immobilize PG in all future assays.

Optimal Ratio of HSA to PG

A direct sandwich ELISA was performed as described in the Materials and Methods section to determine the optimal ratio of HSA to PG for use in the capture matrix. *E. coli* O157:H7 was used to evaluate the capture of bacteria at the various concentrations of HSA and PG tested.

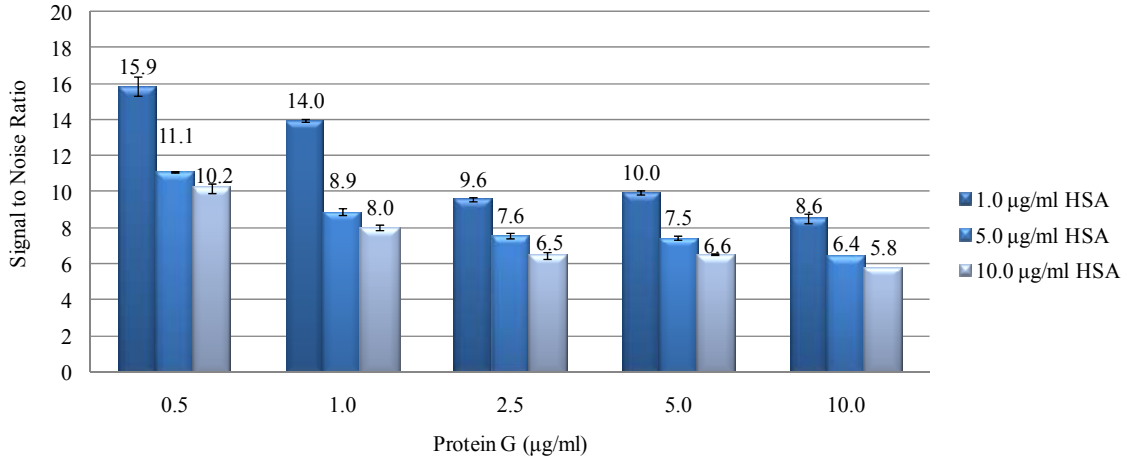

FIGURE 6. Verification of the Optimal Working Ratio of HSA to PG Using ELISA Analysis. Goat polyclonal antibody [1.0 µg/ml], raised against *E. coli* O157:H7, was used

as the primary antibody. Goat polyclonal antibody [1.0 μg/ml], raised against *E. coli* O157:H7 and HRP labeled, was used as the secondary antibody to detect captured *E. coli* O157:H7 at 8.1 x 10^7 CFU/ml. HSA (shown on graph) was used to immobilize PG (shown on graph) before antibodies were added to the assay. Each column, and coinciding standard deviation bar, was calculated from the average of two data points; which were collected from one assay.

A signal to noise ratio greater than 2 was produced by all wells that contained HSA and PG (Figure 6). The signal to noise ratio was greatest when the concentration of PG was 0.5 μg/ml and HSA was 1.0 μg/ml. The signal to noise ratio decreased as the concentration of both HSA and PG increased. These data suggested that the optimal working ratio of HSA to PG was 2:1. This ratio was implemented in all future assays.

The Role of HSA in the Alternative Capture Matrix

Indirect ELISAs were performed as described in the Materials and Methods section to clarify the role of HSA in the capture matrix. The immobilization of antibodies by PG alone, or in combination with HSA, was compared to determine the importance of HSA in the alternative capture matrix.

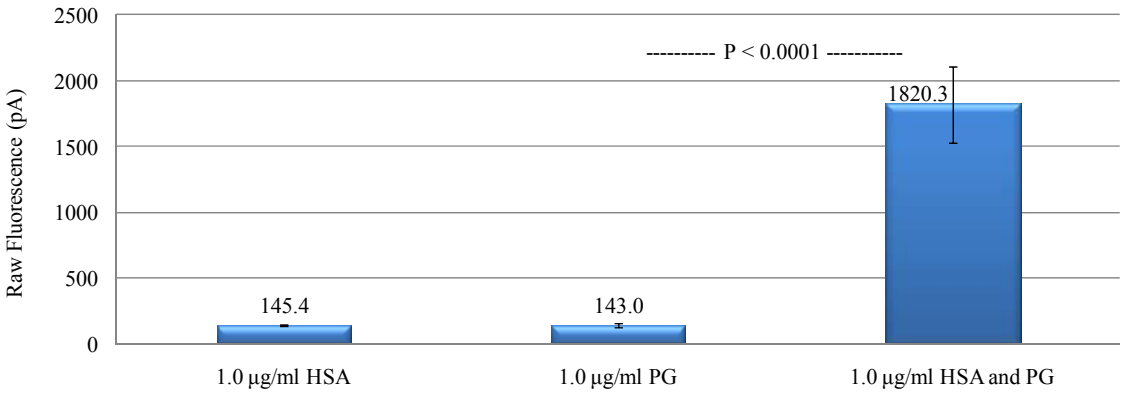

FIGURE 7. The Role of HSA in the Alternative Capture Matrix Clarified Using ELISA Analysis. Rabbit polyclonal antibody [1.0 µg/ml], raised against goat immunoglobulin, was used as the primary antibody; while mouse monoclonal antibody [0.1 µg/ml], raised against rabbit immunoglobulin and HRP labeled, was used as the secondary antibody. Each column, and coinciding standard deviation bar, was calculated from the average of six data points; which were collected from three independent assays.

Minimal fluorescence was produced by wells that contained HSA alone (145.4 pA) and PG alone (143.0 pA) (Figure 7). These data indicated that the primary or secondary antibodies did not bind to the HSA alone or PG alone. The greatest fluorescence was produced by wells that contained HSA and PG (1820.3 pA) in complex. The combination of HSA and PG significantly enhanced the fluorescence signal when compared to HSA alone and PG alone. The primary and secondary antibodies used in the assay were not specific for PG. However, these nonspecific antibodies produced the greatest fluorescence (1820.3 pA) when used to label PG, which was immobilized by HSA. This suggested that the PG Fc binding domain bound to the Fc domain of at least

one of the antibodies used. As indicated by these data, an enhanced ability to immobilize antibodies existed when PG was oriented on a HSA coated surface.

The Role of HSA in Capturing Bacteria

Direct sandwich ELISAs were performed as described in the Materials and Methods section to clarify the role of HSA in the capture of bacteria. *E. coli* O157:H7 was used to show the capture of bacteria by HSA, PG or a combination of HSA and PG.

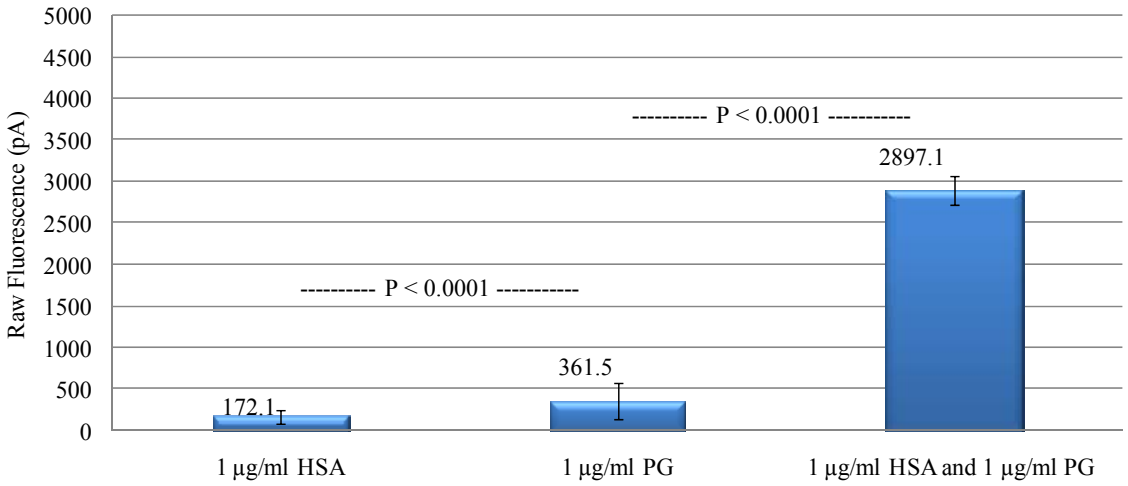

FIGURE 8. The Role of HSA in Capturing Bacteria Clarified Using ELISA Analysis. Goat polyclonal antibody [1.0 µg/ml], raised against *E. coli* O157:H7, was used as the capture antibody and primary detector antibody. Mouse monoclonal antibody [0.1 µg/ml], raised against goat immunoglobulin and HRP labeled, was used as the secondary detector antibody to detect captured *E. coli* O157:H7 at 4.7 x 10^6 CFU/ml. Each column, and coinciding standard deviation bar, was calculated from the average of six data points; which were collected from three independent assays.

Minimal fluorescence (172.1 pA) was produced by wells that contained HSA alone, which indicated that bacteria was not captured by HSA (Figure 11). Significantly ($P < 0.05$) elevated fluorescence was produced by wells that contained PG alone (361.5 pA). The increased fluorescence by PG alone was minor, compared to the fluorescence produced by wells that contained the HSA and PG complex (2897.1 pA). PG, in combination with HSA, was able capture bacteria significantly ($P < 0.05$) better than HSA or PG alone. The HSA-PG combination was implemented in all future assays.

Species Specificity of the Fc Binding Domain

The species specificity of the PG Fc binding domain was explored using competitive ELISAs as described in the Materials and Methods section. One species of antibody, labeled with HRP, was forced to compete for the Fc binding domain on PG with an equal concentration of unlabelled antibody from another species. This competition was performed to demonstrate the strong affinity of the PG Fc binding domain for goat antibodies, and a lesser affinity for mouse antibodies, which had been shown in previous research (1, 4, 14,).

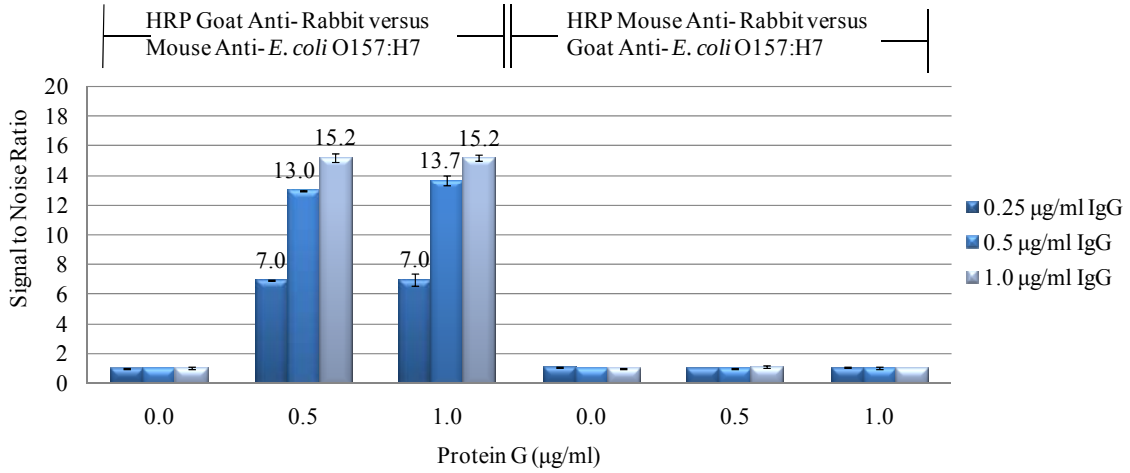

FIGURE 9. Verification of Species Specificity for the Fc Binding Domain of PG Using ELISA Analysis. Goat polyclonal antibody [1.0 µg/ml], raised against *E. coli* O157:H7 and unlabeled, or raised against rabbit immunoglobulin and HRP labeled, was used to compete with mouse monoclonal antibodies for the Fc binding domain of PG [1.0 µg/ml], raised against rabbit immunoglobulin and HRP labeled, or raised against *E. coli* O157:H7 and unlabeled. HSA [1.0 µg/ml] was used to immobilize PG before the antibodies were added. Each column, and coinciding standard deviation bar, was calculated from the average of six data points; which were collected from three independent assays.

Signal to noise ratios greater than 2 were produced by all wells that contained PG and HRP labeled goat polyclonal antibody raised against rabbit immunoglobulin, with unlabeled mouse monoclonal antibody raised against *E. coli* O157:H7. This data indicated that the goat species antibody was the stronger competitor for the Fc binding domain of PG (Figure 9). Signal to noise ratios less than 2 were produced by all wells that contained HRP labeled mouse monoclonal antibody raised against rabbit immunoglobulin, with unlabeled goat polyclonal antibody raised against *E. coli*

O157:H7. This data indicated that the Fc binding domain of PG had minimal affinity for the mouse species antibody. These data corroborated the strong affinity of PG Fc binding domain for the goat antibodies, and the weak binding of mouse antibodies to PG, as stated in previous studies (1, 4, 14).

Optimal Capture Antibody Species

The abilities of rabbit and goat polyclonal antibodies to bind to the Fc binding domain on PG were compared to determine the optimal species of capture antibody for use in the alternative capture matrix. Indirect ELISAs were performed as described in the Materials and Methods section.

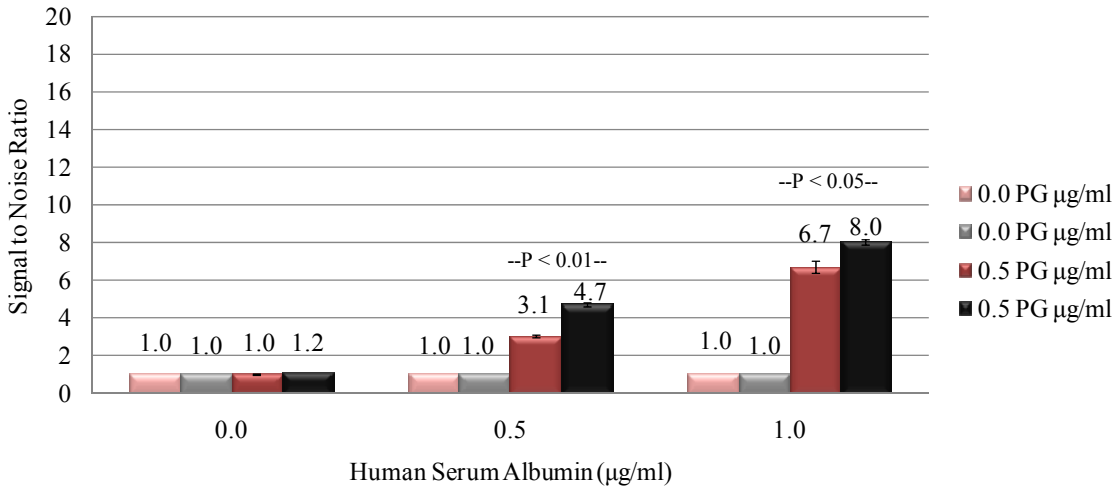

FIGURE 10. Determination of the Optimal Capture Antibody Species Using ELISA Analysis. Goat polyclonal antibody (/), raised against *E. coli* O157:H7, or rabbit polyclonal antibody (/) raised against goat immunoglobulin, were used as primary antibodies [1.0 µg/ml]. Mouse monoclonal antibodies raised against goat or

rabbit immunoglobulin, and HRP labeled, were used as the secondary antibodies [0.1 μg/ml], respectively. HSA (shown on graph) was used to immobilize PG (shown on graph) before antibodies were added to the assay. Each column, and coinciding standard deviation bar, was calculated from the average of six data points; which were collected from three independent assays.

Signal to noise ratios greater than 2 were produced by all wells that contained PG and HSA. These data indicated that rabbit and goat polyclonal antibodies bound to the Fc binding domain of PG in the alternative capture matrix (Figure 10). Goat polyclonal antibody raised against *E. coli* O157:H7 produced significantly ($P < 0.05$) higher signal to noise ratios when compared to rabbit polyclonal antibody raised against goat immunoglobulin. These data suggested that goat species antibody was the most effective capture antibody in the alternative capture matrix, when compared to rabbit species antibody. The rabbit species antibody bound to the Fc binding domain of PG, which suggested that it may be effective as a capture antibody if goat species antibody was not readily available for a particular target. Goat polyclonal antibody raised against *E. coli* O157:H7 was implemented as the capture antibody in further assays.

Optimal Concentration of Detector Antibody

Direct sandwich ELISAs were performed as described in the Materials and Methods section. Goat polyclonal antibody, raised against *E. coli* O157:H7 and HRP labeled, was used to determine the optimal concentration of detector antibody for the alternative capture matrix.

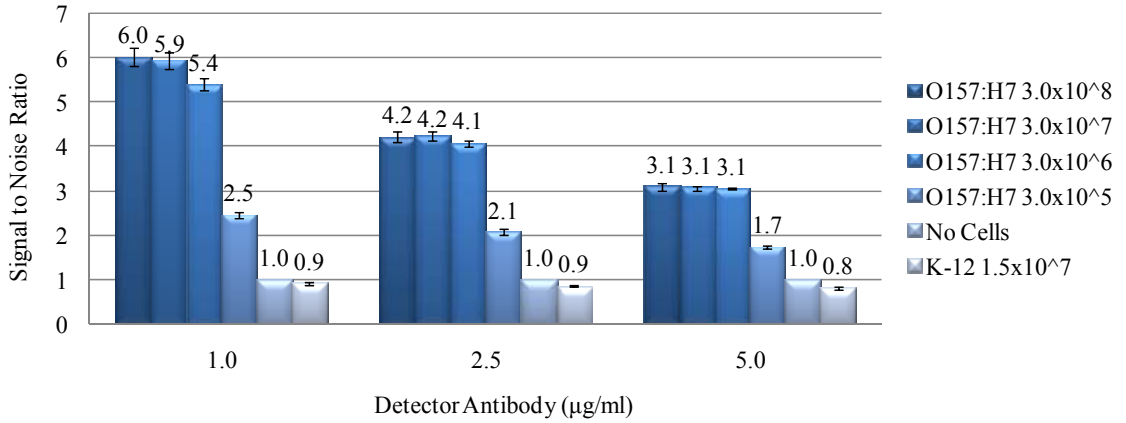

FIGURE 11. Determination of the Optimal Concentration of Detector Antibody Using ELISA Analysis. Goat polyclonal antibody [1.0 µg/ml], raised against *E. coli* O157:H7, was used as the capture antibody. Goat polyclonal antibody [1.0, 2.5, 5.0 µg/ml], raised against *E. coli* O157:H7 and HRP labeled, was used as the detector antibody to detect captured *E. coli* O157:H7 (CFU/ml shown on graph). *E. coli* K-12 [1.5 x 10^7 CFU/ml] was used as a negative control. HSA [1.0 µg/ml] was used to immobilize PG [0.5 µg/ml] before antibodies were added to the assay. Each column, and coinciding standard deviation bar, was calculated from the average of six data points; which were collected from three independent assays.

Signal to noise ratios greater than 2 were produced by all wells that contained *E. coli* O157:H7 at 3.0 x 10^6 through 3.0 x 10^8 CFU/ml (Figure 11). Signal to noise ratios decreased when the concentration of detector antibody increased. These data suggested that saturation of PG began at, or before, 1.0 µg/ml of detector antibody. Based on the greatest signal to noise ratio, the optimal concentration of detector antibody was 1.0 µg/ml or less.

Capture Antibody Displacement

Direct sandwich ELISAs were performed as described in the Materials and Methods section. The absence of *E. coli* O157:H7 was used to determine if the detector antibody, goat polyclonal antibody raised against *E. coli* O157:H7 and HRP labeled, had displaced the capture antibody, goat polyclonal antibody raised against *E. coli* O157:H7, for the Fc binding domain on PG.

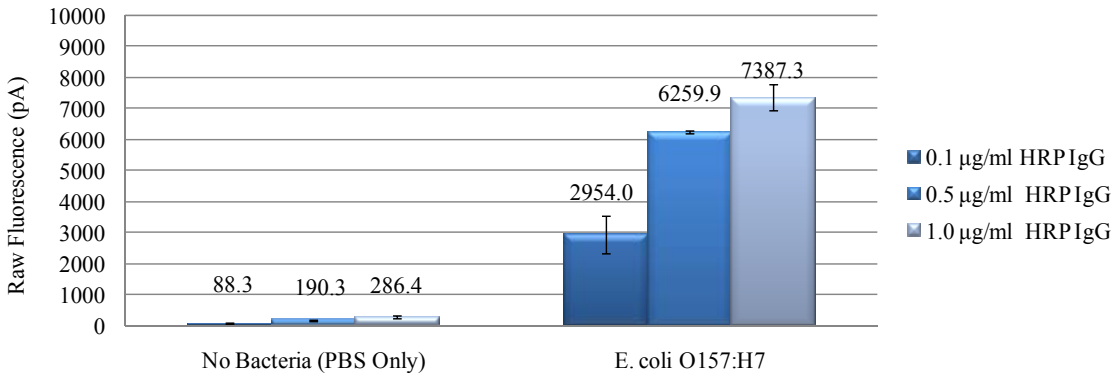

FIGURE 12. Capture Antibody Displacement Evaluated Using ELISA Analysis. Goat polyclonal antibody [1.0 µg/ml], raised against *E. coli* O157:H7, was used as the capture antibody. Goat polyclonal antibody [0.1, 0.5 or 1.0 µg/ml], raised against *E. coli* O157:H7 and HRP labeled, was used as the detector antibody, to detect captured *E. coli* O157:H7 [9.7 x 10^6 CFU/ml]. The absence of bacteria was used as the negative control. HSA [1.0 µg/ml] was used to immobilize PG [0.5 µg/ml] before antibodies were added to the assay. Each column, and coinciding standard deviation bar, was calculated from the average of six data points; which were collected from three independent assays.

Fluorescence above 2000 pA was produced by all wells that contained *E. coli* O157:H7 (Figure 12). These data indicated that the alternative capture matrix captured

the targeted cells. In the presence of bacteria, fluorescence signals were not increased significantly ($P < 0.05$) when the concentration of detector antibody was increased. This lack of signal increase suggested that the antigen binding sites were saturated by detector antibody at 0.5 µg/ml. Minimal fluorescence (< 700 pA) was produced by all wells that lacked bacteria. These data indicated that the detector antibody, at 0.5 and 1.0 µg/ml, did not bind to PG. This lack of binding suggested that the detector antibody did not displace the capture antibody from the Fc binding domain of PG. Goat polyclonal antibody raised against *E. coli* O157:H7 and HRP labeled was implemented as the detector antibody in all future ELISAs.

Limit of Detection for Two Capture Matrices Using ELISA Analysis

Direct sandwich ELISAs were performed as described in the Materials and Methods section. The streptavidin-biotin and HSA-PG capture matrices were compared to determine the limit of detection for *E. coli* O157:H7.

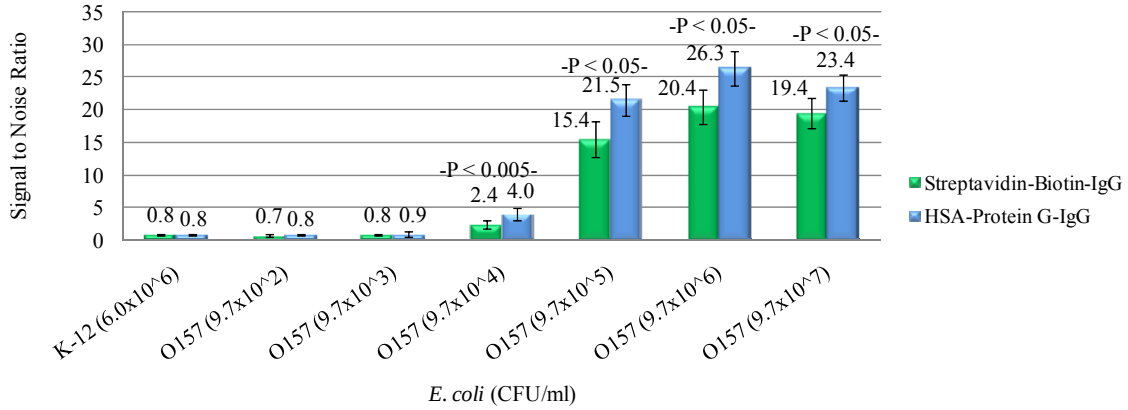

FIGURE 13. Determination of the Limit of Detection for Two Capture Matrices Using ELISA Analysis. Goat polyclonal antibodies [1.0 µg/ml], raised against *E. coli* O157:H7

and unlabeled or biotinylated, were used as the capture antibody. Goat polyclonal antibody [1.0 μg/ml], raised against *E. coli* O157:H7 and HRP labeled, was used as the detector antibody, to detect captured *E. coli* O157:H7 (CFU/ml shown on graph). *E. coli* K-12 (CFU/ml shown on graph) was used as the negative control. HSA [1.0 μg/ml] was used to immobilize PG [0.5 μg/ml], before antibodies were added to the HSA-PG matrix. Streptavidin [1.0 μg/ml] was used to immobilize the biotinylated capture antibody, before bacteria were added to the assay. Each column, and coinciding standard deviation bar, was calculated from the average of six data points; which were collected from three independent assays.

Signal to noise ratios less than 2 were produced by all wells that contained the negative control, *E. coli* K-12. These data indicated that *E. coli* K-12 was not detected by either capture matrix. Signal to noise ratios greater than 2 were produced by all wells that contained *E. coli* O157:H7, from 9.7×10^4 through 1×10^7 CFU/ml. This high signal to noise ratio indicated that the limit of detection for *E. coli* O157:H7 was 9.7×10^4 CFU/ml for both capture matrices using ELISA analysis. The HSA-PG capture matrix produced signal to noise ratios that were significantly higher than the streptavidin-biotin capture matrix, at every concentration of *E. coli* O157:H7. These data suggested that the HSA-PG capture matrix was a better method for the capture of target bacterial cells using ELISA analysis.

The Limit of Detection of Two Capture Matrices Using RAPTOR

RAPTOR assays, using a sandwich assay format, were performed as described in the Materials and Methods section. Experiments were conducted to compare the detection limit of the streptavidin-biotin-IgG capture matrix to the HSA-PG-IgG capture matrix. GFP-*E. coli* O157:H7 was used to show the capture of bacteria by these matrices.

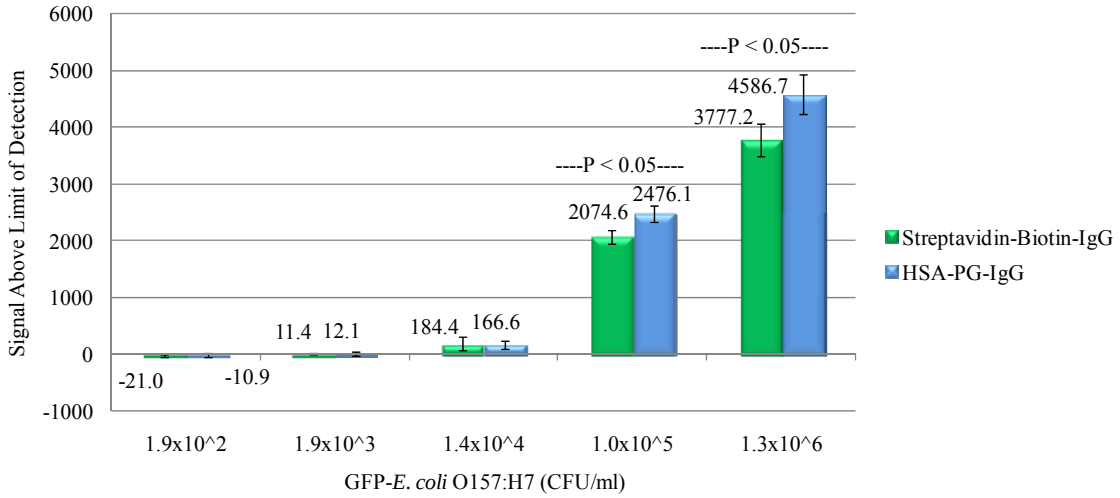

FIGURE 14. Determination of the Limit of Detection for Two Capture Matrices Using RAPTOR Analysis. Goat polyclonal antibodies [50.0 µg/ml], raised against *E. coli* O157:H7 and unlabeled or biotinylated, were used as the capture antibody. Goat polyclonal antibody [5.0 µg/ml], raised against *E. coli* O157:H7 and Cy5 labeled, was used as the detector antibody, to detect captured GFP-*E. coli* O157:H7 (CFU/ml shown on graph). HSA [100.0 µg/ml] was used to immobilize PG [50.0 µg/ml], before antibodies were added to the HSA-PG matrix. Streptavidin [100.0 µg/ml] was used to immobilize the biotinylated capture antibody, before bacteria were added to the assay. Each column, and coinciding standard deviation bar, was calculated from the average of two data points from 1.0 x 10^5 and 1.0 x 10^6 CFU/ml, six data points from 1.4 x 10^4

CFU/ml, and eight data points from 1.9 x 10^2 and 1.9 x 10^3 CFU/ml; which were collected from five independent assays.

Positive SALOD values were produced by waveguides used to assay 1.9 x 10^3 through 1.3 x 10^6 CFU/ml of GFP-*E. coli* O157:H7 (Figure 14). These data indicated that the limit of detection for both matrices was 1.9 x 10^3 CFU/ml. No significant difference was observed between the two matrices at 1.9 x 10^2 through 1.4 x 10^4 CFU/ml of GFP-*E. coli* O157:H7. These data indicated that both matrices captured the target bacteria for detection below 1.0 x 10^5 CFU/ml, and produced similar SALOD values. The HSA-PG capture matrix produced significantly ($P < 0.05$) greater SALOD values at 1.0 x 10^5 through 1.3 x 10^6 CFU/ml; when compared to the streptavidin-biotin capture matrix. These data suggested that the HSA-PG capture matrix was the better method for capture of target bacterial cells at high concentrations using the RAPTOR.

The Limit of Detection for Ground Beef Homogenate Supernatant

RAPTOR assays, using a sandwich format with direct detection, were performed as described in the Materials and Methods section. Ground beef homogenate supernatant fluid, containing *E. coli* O157:H7, was used to compare the HSA-PG and streptavidin-biotin capture matrices for use in an animal-based food sample.

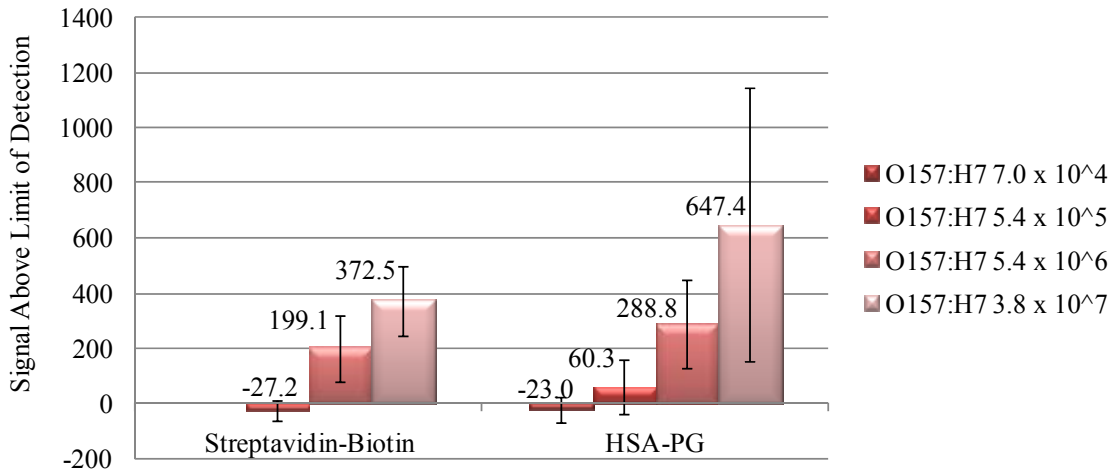

FIGURE 15. Determination of the Limit of Detection for Two Capture Matrices in Homogenized Ground Beef Supernatant Fluid Using RAPTOR Analysis. Goat polyclonal antibodies [50.0 µg/ml], raised against *E. coli* O157:H7 and unlabeled, or biotinylated, was used as the capture antibody. Goat polyclonal antibody [5.0 µg/ml], raised against *E. coli* O157:H7 and Cy5 labeled, was used as the detector antibody, to detect captured *E. coli* O157:H7 (CFU/ml shown on graph). HSA [100.0 µg/ml] was used to immobilize PG [50.0 µg/ml], before antibodies were added to the HSA-PG matrix. Streptavidin [100.0 µg/ml] was used to immobilize the biotinylated capture antibody before bacteria were added to the assay. Each column, and coinciding standard deviation bar for the HSA-PG capture matrix, was calculated from the average of two data points for 7.0 x 10^4 CFU/ml, seven data points from 5.4 x 10^5 and 5.4 x 10^6 CFU/ml, and three data points for 3.8 x 10^7 CFU/ml; which were collected from three independent assays. Each column, and coinciding standard deviation bar for the streptavidin-biotin capture matrix, was calculated from the average of three data points; which were collected from three independent assays. The streptavidin-biotin capture matrix was not tested at the 7.0 x 10^4 CFU/ml sample concentration.

Positive SALOD values were produced by all waveguides treated with the HSA-PG and 5.4 x 10^5 CFU/ml of *E. coli* O157:H7 (Figure 15). All waveguides treated with streptavidin-biotin produced positive SALOD values at 5.4 x 10^6 CFU/ml of *E. coli* O157:H7; which was one log less sensitive when compared to the HSA-PG capture matrix. For each bacterial concentration, SALOD values were not significantly ($P > 0.05$) greater for the HSA-PG capture matrix, when compared to the streptavidin-biotin capture matrix. These data indicated that the HSA-PG capture matrix was the better method used to capture target bacteria in beef homogenized supernatant fluid, using the RAPTOR for detection.

The Limit of Detection for Spinach Leaf Homogenate Supernatant

RAPTOR assays, using a sandwich format with direct detection, were performed as described in the Materials and Methods section. Spinach leaf homogenate supernatant fluid containing *E. coli* O157:H7, was used to test the HSA-PG capture matrix in a plant-based food sample.

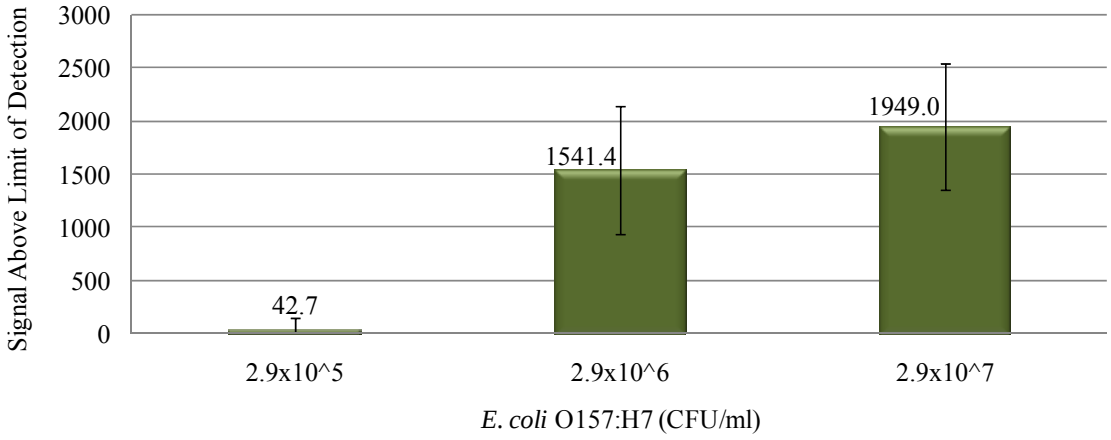

FIGURE 16. Determination of the Limit of Detection for the HSA-PG Capture Matrix in

Homogenized Spinach Leaf Supernatant Fluid Using RAPTOR Analysis. Goat polyclonal antibodies [50.0 μg/ml], raised against *E. coli* O157:H7 and unlabeled, was used as the capture antibody. Goat polyclonal antibody [5.0 μg/ml], raised against *E. coli* O157:H7 and Cy5 labeled, was used as the detector antibody, to detect captured *E. coli* O157:H7 (CFU/ml shown on graph). HSA [100.0 μg/ml] was used to immobilize PG [50.0 μg/ml], before antibodies were added to the HSA-PG matrix. Each column, and coinciding standard deviation bar, was calculated from the average of four data points; which were collected from one assay.

Positive SALOD values were produced for 2.9 x 10^5 CFU/ml *E. coli* O157:H7 (Figure 16). These data suggested that the limit of detection of *E. coli* O157:H7 in spinach homogenate supernatant fluid was 2.9 x 10^5 CFU/ml (Figure 16). SALOD values increased more than two logs when the bacterial concentration was increased by one log, to 2.9 x 10^6 CFU/ml. This unusual increase in signal suggested that the fluorescence detected may have been influenced by a component in the spinach homogenate supernatant fluid. These data suggested that the SALOD values obtained were not accurately interpreted by the RAPTOR assay.

The Capture Efficiency for Two Capture Matrices on Waveguide Surfaces

The capture efficiency of the HSA-PG capture matrix was compared to the capture efficiency of the streptavidin-biotin capture matrix using GFP-*E. coli* O157:H7. RAPTOR assays were performed using a direct sandwich assay format as described in the Materials and Methods section. After the RAPTOR assays were performed, the

amount of bacterial cells captured on the surfaces of the waveguides was measured using fluorescent microscopy, as described in the Materials and Methods section.

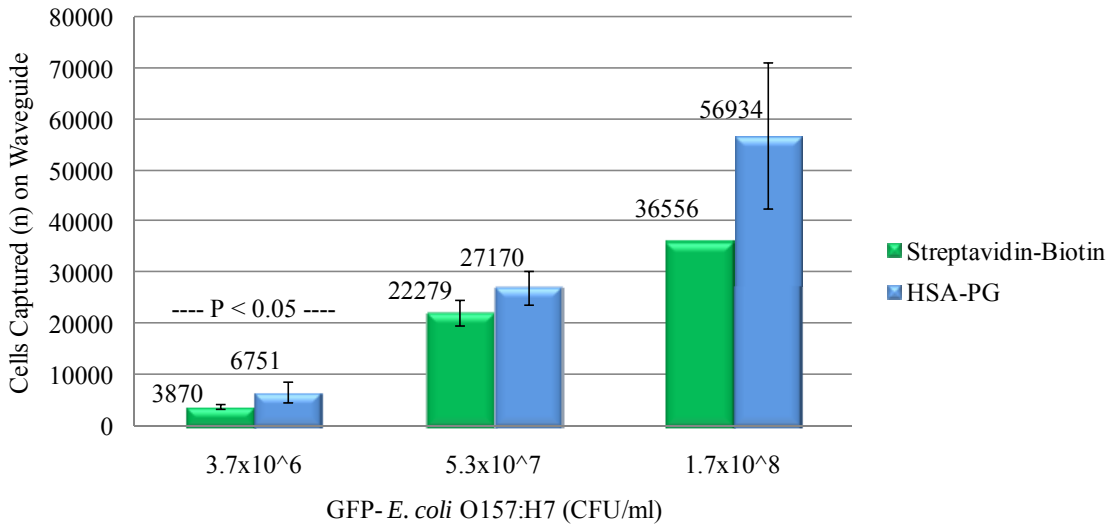

FIGURE 17. Average Numbers of Cells Captured on the Waveguide Surface After RAPTOR Analysis. Goat polyclonal antibodies [50.0 µg/ml], raised against *E. coli* O157:H7 and unlabeled or biotinylated, were used as the capture antibody. Goat polyclonal antibody [5.0 µg/ml], raised against *E. coli* O157:H7 and Cy5 labeled, was used as the detector antibody, to detect captured GFP-*E. coli* O157:H7 (CFU/ml shown on graph). HSA [100.0 µg/ml] was used to immobilize PG [50.0 µg/ml], before antibodies were added to the HSA-PG matrix. Streptavidin [100.0 µg/ml] was used to immobilize the biotinylated capture antibody before bacteria were added to the assay. Each column, and coinciding standard deviation bar, was calculated from the average of six data points for 3.7 x 10^6 CFU/ml, four data points for 5.3 x 10^7 CFU/ml; which were collected from six independent assays. Each column, and coinciding standard deviation bar, was calculated from the average of three data points for 1.7 x 10^8 CFU/ml using the

HSA-PG matrix and one data point for 1.7 x 10^8 CFU/ml using the streptavidin biotin matrix; which were collected from three independent assays.

The average number of cells manually counted in each viewable field on the surface of waveguides ranged from seven for sample concentrations of 3.7 x 10^6 CFU/ml, to over four hundred for sample concentrations of 1.7 x 10^8 CFU/ml. Waveguides treated with the HSA-PG capture matrix retained twice the amount of cells, when compared to the streptavidin-biotin capture matrix, at 3.7 x 10^6 CFU/ml; which was a significantly ($P < 0.05$) greater amount (Figure 17). Waveguides treated with the HSA-PG capture matrix failed to significantly improve the amount of cells captured on the waveguide surface, when compared to waveguides treated with the streptavidin-biotin capture matrix from 5.3 x 10^7 through 1.7 x 10^8 CFU/ml.

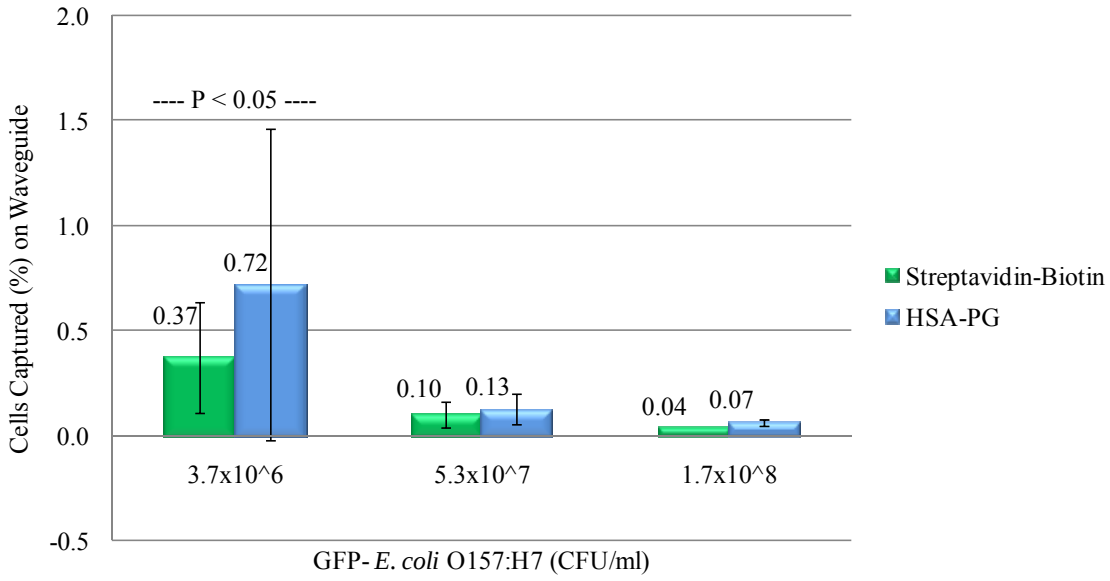

FIGURE 18. Average Capture Efficiency on the Waveguide Surface After RAPTOR Analysis. Goat polyclonal antibodies [50.0 µg/ml], raised against *E. coli* O157:H7 and

unlabeled or biotinylated, were used as the capture antibody. Goat polyclonal antibody [5.0 μg/ml], raised against *E. coli* O157:H7 and Cy5 labeled, was used as the detector antibody, to detect captured GFP-*E. coli* O157:H7 (CFU/ml shown on graph). HSA [100.0 μg/ml] was used to immobilize PG [50.0 μg/ml], before antibodies were added to the HSA-PG matrix. Streptavidin [100.0 μg/ml] was used to immobilize the biotinylated capture antibody before bacteria were added to the assay. Each column, and coinciding standard deviation bar, was calculated from the average of six data points for 3.7×10^6 CFU/ml, four data points for 5.3×10^7 CFU/ml; which were collected from six independent assays. Each column, and coinciding standard deviation bar, was calculated from the average of three data points for 1.7×10^8 CFU/ml using the HSA-PG matrix and one data point for 1.7×10^8 CFU/ml using the streptavidin biotin matrix; which were collected from three independent assays.

The capture efficiency (%) was greatest at 3.7×10^6 CFU/ml, and decreased as the sample concentration increased, for both capture matrices. The HSA-PG capture matrix showed significantly ($P < 0.05$) greater capture efficiency when compared to streptavidin-biotin for 3.7×10^6 CFU/ml. At sample concentrations from 5.3×10^7 through 1.7×10^8 CFU/ml, the waveguides treated with the HSA-PG capture matrix failed to significantly increase the capture efficiencies of GFP-*E. coli* O157:H7 on waveguide surfaces, when compared to waveguides treated with the streptavidin-biotin matrix.

A Comparison of DyLight™649 and Cy5 Labeled Detector Antibody

Attainment of a lower limit of detection for the HSA-PG capture matrix was attempted by testing an alternative detection fluorophore. The DyLight™649 fluorophore has been reported by the manufacturer as being more photo stable than the Cy5 fluorophore. RAPTOR assays were performed, using a direct sandwich format, as described in the Materials and Methods section, to compare detection limits of Cy5, and DyLight™649 labeled detector antibodies. GFP-*E. coli* O157:H7 was used to show the detection of bacteria using waveguides treated with the HSA-PG capture matrix.

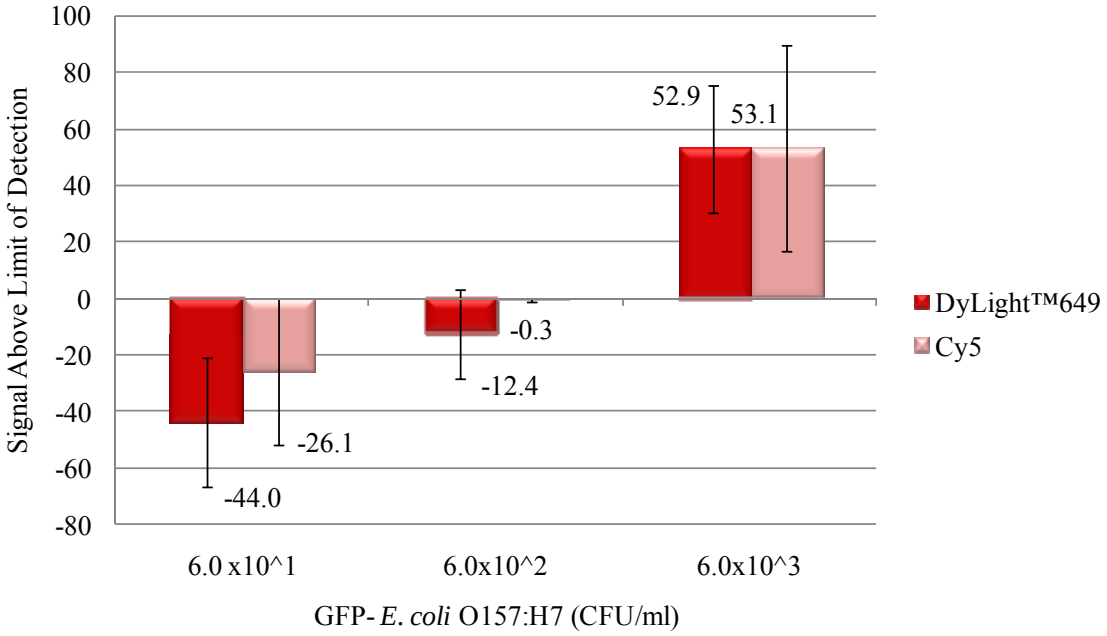

FIGURE 19. A Comparison of DyLight™649 and Cy5 Labeled Detector Antibody Using RAPTOR Analysis. Goat polyclonal antibodies [50.0 µg/ml], raised against *E. coli* O157:H7 and unlabeled, was used as the capture antibody. Goat polyclonal antibodies [5.0 µg/ml], raised against *E. coli* O157:H7 and DyLight™649 or Cy5 labeled, was used as the detector antibody, to detect captured GFP-*E. coli* O157:H7 (CFU/ml shown on

graph). HSA [100.0 μg/ml] was used to immobilize PG [50.0 μg/ml], before antibodies were added to the HSA-PG matrix. Each column, and coinciding standard deviation bar, was calculated from the average of three data points; which were collected from two independent assays.

A significant ($P > 0.05$) difference was not found between the SALOD values produced from DyLight™649 and Cy5 labeled detector antibodies, for all sample concentrations tested (Figure 19). The limit of detection was the same for 6.0×10^3 CFU/ml, for both fluorophores tested. These data suggested that the use of DyLight™649 labeled detector antibodies failed to increase the sensitivity of the RAPTOR assay, when compared to the use of Cy5 labeled detector antibodies, to detect *E. coli* O157:H7.

DISCUSSION

An alternative method for immobilizing capture antibody on an immunoassay surface was explored, after existing strategies were researched (5, 6, 11, 15, 16, 19, 22, 23, 24, 31, 34, 35, 39, 40). One common strategy for securing capture antibodies to a polystyrene surface is to passively adsorb streptavidin to the surface. The streptavidin coated surface is then used to bind biotinylated capture antibodies. This binding is incredibly strong (13), and resists denaturation of the immobilized antibody (39), which led to a broad acceptance for this method (6, 19, 23, 36) in the field of microbiology and immunology. Biotinylation of the antibody is done by a covalent interaction targeted towards primary amines, which are located on the constant and variable regions of the antibody heavy chain. When the biotinylated antibody is incubated on the streptavidin coated surface the immobilization results in a random orientation of the antibodies (24, 31). This lack of uniformity, of the biotinylated antibody may cause poor sensitivity (3, 24), which currently plagues immunoassays (6, 19, 23, 36). To test this reasoning, an alternative capture matrix was constructed and then compared to the streptavidin-biotin matrix.

The most abundant form of streptococcal PG, available on the commercial market, is a recombinant PG, which lacks an albumin binding domain (14 kDa); which is located near the amine terminus. Recombinant PG is commonly employed to remove antibodies from serum without nonspecifically binding to the albumin present. This common use of the recombinant form of PG led to a minimal demand for the native form

of PG. For this research, obtaining native PG with an intact and functional albumin binding domain was essential. This native form of PG has limited commercial availability; and only one company, Calbiochem, was located that sold the native protein, with the intact albumin binding domain. Validation of the presence and functionality of the albumin binding domain in this product was the first step performed to construct the alternative capture matrix. In the presence of HSA, Figure 4 shows the functionality of the albumin binding domain in native PG, by the production of signal to noise ratios greater than the signal to noise ratios produced by recombinant PG. These results indicated that native PG had a functional albumin binding domain able to bind HSA. These results also indicated that recombinant PG did not have a functional albumin binding domain, and was not able to bind to HSA. The use of native PG was implemented for all future assays.

Different species of albumin were tested to determine the species specificity of the albumin binding domain of PG. The albumin species tested were chosen based on a previous study (25); which showed that human, rabbit and bovine serum inhibited the Fc binding of radiolabeled human species antibodies to bacterial cells from group G and C streptococci. This binding inhibition suggested that the radiolabeled antibodies were displaced by competitive antibodies present in the serum. This inhibition did not occur when chicken, rat, dog and cat serum were tested (25). The Fc binding domain of PG was shown to bind to rabbit and human species antibody (4), but did not bind to chicken species antibody (14). This pattern of species specificity demonstrated by the Fc binding domain led to the reasoning that the specificity may be transferrable to the albumin

binding domain. To test this theory, PG was immobilized by human serum albumin (HSA), bovine serum albumin (BSA), or chicken ovalbumin (OVA).

Minimal signal to noise ratios were produced by wells that contained OVA, which indicated that OVA did not immobilize PG (Figure 5). Signal to noise ratios greater than two were produced by wells that contained 5.0 μg/ml of BSA, which indicated that high concentrations of BSA did immobilize PG. Interaction between BSA and PG was important to consider because many laboratory reagents, such as antibodies, contain nominal concentrations of BSA as a stabilizing agent. These results indicated that small amounts of BSA in the reagents did not interfere with the assays using the HSA-PG capture matrix. HSA showed the greatest binding to PG, even at minimal concentrations, which indicated that human was the optimal species of albumin for use in the alternative capture matrix. As theorized, the species specificity shown by the Fc binding domain was also shared by the albumin binding domain. Further studies, using rabbit, goat, and mouse sera, are needed to explore the relationship between species specific domains on multi-functional proteins, and to find a superior albumin species to immobilize PG, to assay surfaces.

A range of concentrations of PG and HSA were tested to determine the optimal working ratio of these two components in the alternative capture matrix. Figures 4 and 5 compare the concentrations of HSA and PG without the presence of bacteria. Based on the greatest signal to noise ratios, Figure 4 shows the optimal concentration of HSA was 1.0 μg/ml, and PG was 0.5 μg/ml. Figure 5 shows the greatest signal to noise ratios at 5.0 μg/ml for HSA, and 2.5 μg/ml for PG. Higher concentrations showed greater signal to noise ratios, but the ratio of the components was identical, at 2.0 μg/ml of HSA for every

1.0 μg/ml PG. *E. coli* O157:H7 was added to the experiment to verify that this ratio was optimal in the presence of bacteria and to better anticipate the activity of these components during a working immunoassay. Figure 6 shows the signal to noise ratios for 1.0 μg/ml of HSA and 0.5 μg/ml of PG. The 2:1 ratio produced the greatest signal to noise ratios, using the lower concentrations of HSA and PG to capture *E. coli* O157:H7. This 2:1 ratio of HSA and PG was implemented for all future assays.

In previous studies, fragments of PG or intact PG, have been used to immobilize capture antibodies on assay surfaces in immunoassays (3, 18, 40). Methods to secure PG to the assay surface, e.g., amine or thiol reactive chemistry (3, 40), have improved antibody activity, when compared to direct adsorption. Covalent attachment of the albumin binding domain of PG to Fab fragments has further improved antibody activity, by immobilizing the antibody on a HSA coated surface (18). In this study, the role of HSA in the alternative capture matrix was clarified by comparing antibody immobilization using HSA, PG or HSA-PG combined.

Figure 7 shows antibodies immobilized by HSA alone, PG alone, and PG and HSA combined, in the absence of bacteria. Minimal fluorescence was produced by HSA alone and PG alone which indicated that the antibodies were not immobilized. The combination of HSA and PG produced the greatest fluorescence, which was significantly ($P < 0.05$) greater than the fluorescence produced by PG alone or HSA alone. The antibodies used were not specific for HSA or PG so any binding was via the Fc domain, which constituted non-immune binding; and not via the antibody paratopes, which are used for immune binding. This improved fluorescence indicated that a greater amount of primary antibody was immobilized by PG when PG was immobilized by HSA. As shown

in a previous study, the greater density of immobilized antibody contributed to greater sensitivity of the assay when a target was introduced (24). *E. coli* O157:H7 was introduced into the experiment to test this theory using the alternative capture matrix.

Figure 8 shows minimal fluorescence produced by HSA alone, which indicated that *E. coli* O157:H7 was not captured by HSA alone. Significantly greater fluorescence was produced by PG alone, which suggested that PG immobilized capture antibody and bacteria for detection. The greatest fluorescence was produced by HSA and PG combined, when compared to fluorescence produced by PG or HSA alone. When PG was immobilized by an albumin coated surface, the Fc binding domain was available to bind antibodies in the environment. Previous study has shown that the structure of PG consists of structurally opposite Fc and albumin binding domains. PG was able to bind an antibody molecule and an albumin molecule at the same time, without allosteric modulation (7). This strict orientation of antibody, by the Fc binding domain, allowed for a greater incidence of antibody binding, when compared to PG passively adsorbed to a non-albumin coated surface; which resulted in random orientation of the PG (27). The greater availability of the Fc binding domain was characterized by a greater density of capture antibody; which resulted in the enhanced capture of *E. coli* O157:H7. The use of PG immobilized by HSA was implemented for all future assays.

The optimal species of antibody for use as capture and detector antibody was determined for use in the alternative capture matrix. Figure 9 and 10 show the results of a series of competitive ELISAs used to investigate the species specificity of the Fc binding domain of PG. In Figure 9, competitive ELISAs were used to compare goat and mouse antibodies. Signal to noise ratios greater than 6 were produced by all wells that contained

HRP labeled goat antibodies, and unlabeled mouse antibodies. These results indicated that the goat antibodies were stronger competitors for the Fc binding domain of native PG. The success of goat antibody in competing for the Fc binding domain of PG suggested that goat species antibody was a prime candidate for use as the capture antibody in the alternative capture matrix. Signal to noise ratios less than 2 were produced by all wells that contained HRP labeled mouse antibodies and unlabeled goat antibodies. These results indicated that the HRP labeled mouse antibody failed to compete for Fc binding domain of PG. This failure suggested that mouse species antibody should not be implemented as a capture antibody in the alternative capture matrix. A previous study reported similar findings as shown in Table 2 (14). Nearly five times the amount of mouse polyclonal antibody (1020 ng) was required to produce fifty percent inhibition of binding between the Fc binding domain of PG and rabbit polyclonal antibody, when compared to only 217 ng of goat polyclonal antibody, required to produce the same inhibition. The greater requirement for mouse antibody, compared to goat antibody, suggested that the Fc binding domain of PG had greater affinity for goat species antibody (14). These results led to the potential use of mouse antibody as a detector antibody; while goat species antibody was implemented as the capture antibody in the developing capture matrix.

Further species specificity analysis of the Fc binding domain was warranted to investigate alternative capture antibodies for use in the alternative capture matrix. Table 2 shows the similar affinity of PG for rabbit and goat species antibody. Polyclonal goat and rabbit antibodies were compared using indirect ELISAs. To avoid competitive binding to PG, indirect detection was performed by HRP labeled mouse antibodies, which were

raised against goat or rabbit antibodies. Figure 10 shows signal to noise ratios that were significantly ($P < 0.05$) greater for wells that contained goat antibodies, when compared to wells that contained rabbit antibody. These results suggested that goat species antibody was the preferred candidate for use as a capture antibody. Rabbit antibodies showed the second highest affinity for the Fc binding domain of PG, and could therefore potentially be employed as an alternative capture antibody in the event that a goat species antibody is not readily available for a particular antigen. Since PG showed high affinity for the goat polyclonal antibody raised against *E. coli* O157:H7, and since it is specific and sensitive for *E. coli* O157:H7, it was used as the capture antibody in all future assays.

The species and concentration of the detector antibody was important to consider when PG was used in an immunoassay format. PG has previously shown a range of affinities for different species of antibody (1, 4, 14). However, PG has not shown a high affinity towards chicken (1, 14) or mouse (1, 4) antibodies, which suggested that they could be used as detector antibodies. HRP labeled chicken and mouse antibodies, raised against *E. coli* O157:H7, were tested for use as detector antibodies, but were found to be insensitive and non-specific for the target organism; when compared to goat antibodies raised against *E. coli* O157:H7 (data not shown). Goat polyclonal antibodies raised against *E. coli* O157:H7 were implemented as the capture and detector antibody for all future assays.

Further investigation was required to avoid displacement of the goat species capture antibodies on PG by the goat species detector antibodies, which the Fc binding domain has similar affinity for. In Figure 11, 1.0 μg/ml of detector antibody produced the greatest signal to noise ratios at all concentrations of *E. coli* O157:H7. Due to elevated

background signals, the signal to noise ratios decreased as the concentration of detector antibody increased. These results suggested that the excess detector antibody may have displaced the same-species capture antibody. To test for displacement of the capture antibody by the detector antibody fluorescence values produced by wells that contained bacteria were compared to fluorescence values produced wells that lacked bacteria. Figure 12 shows that when *E. coli* O157:H7 was absent from the environment, minimal fluorescence (< 300 pA) was produced, which indicated that the detector antibody did bind due to a lack of target. These results also indicated that the detector antibody did not bind to the PG present in the capture matrix, and that the Fc binding domains were effectively saturated with the capture antibody. The lack of fluorescence further indicated that the capture antibodies at 1.0 μg/ml was not displaced by the same-species detector antibodies, at 0.1 μg/ml through to 1.0 μg/ml. Goat species detector antibody at 1.0 μg/ml was implemented for all future assays using ELISA analysis.

Sensitivity of the immunoassay was a major consideration during the development of the alternative capture matrix. The limit of detection was used as a measure of sensitivity, which was based on the concentration of bacteria captured and subsequently detected by the immunoassay. Figure 13 shows the limit of detection was 9.7×10^4 CFU/ml for *E. coli* O157:H7 by the streptavidin-biotin and the HSA-PG capture matrices. The HSA-PG capture matrix produced signal to noise ratios significantly ($P < 0.05$) greater than the streptavidin-biotin capture matrix for all bacterial concentrations tested greater than 9.7×10^3 CFU/ml. The most significant difference produced between the capture matrices was for the lowest sample concentration, 9.7×10^4 CFU/ml. As the concentration of bacteria increased, the difference in signal to noise ratios decreased

between the two capture matrices. These results suggested that the bacterial target began to saturate the antigen binding sites for both matrices at 9.7 x 10^5 CFU/ml.

The sensitivity of the two capture matrices was compared using RAPTOR analysis. Figure 14 shows the same sensitivity, or limit of detection, for the two capture matrices (streptavidin-biotin and HSA-PG) at 1.9 x 10^3 CFU/ml of *E. coli* O157:H7. At sample concentrations below 1.0 x 10^5 CFU/ml, a significant ($P < 0.05$) difference was not produced between the two capture matrices. These results indicated that at lower concentrations of *E. coli* O157:H7 the sensitivity was not improved by the HSA-PG capture matrix. The HSA-PG capture matrix produced significantly ($P < 0.05$) greater SALOD values for 1.0 x 10^5 through 1.3 x 10^6 CFU/ml, when compared to the streptavidin-biotin capture matrix. The increased SALOD values suggested the enhanced capture of bacteria in samples with concentrations greater than 1.0 x 10^5 CFU/ml of *E. coli* O157:H7.

The amount of bacteria captured on the waveguide surface was quantified to compare the capture efficiency of the two capture matrices. Figure 17 shows that the greatest amount of GFP-*E. coli* O157:H7 captured was by the HSA-PG matrix, when compared to the streptavidin-biotin matrix at all concentrations tested. The number of cells counted on the HSA-PG waveguides was significantly ($P < 0.05$) greater when compared to the streptavidin-biotin treated waveguides, exclusively at low bacterial concentrations (3.7 x 10^6 CFU/ml). At higher concentrations, the amount of cells captured by the two matrices was not significantly ($P < 0.05$) different. Figure 18 shows the measured capture efficiency was 0.37% for the streptavidin-biotin capture matrix, and 0.72% for the HSA-PG capture matrix, when GFP-*E. coli* O157:H7 was assayed at 3.7 x

10^6 CFU/ml in a 500 µl sample volume. GFP-*E. coli* O157:H7 was used in a previous study to measure the capture efficiency of the streptavidin-biotin capture matrix, which was reported at 0.54% for 1.0 x 10^6 CFU/ml in an 800 µl sample volume (36). This difference in capture efficiency for the streptavidin-biotin capture matrix could have been due to the change in sample volume, which was unavoidable due to a limitation in the equipment used. Capture efficiency was an invaluable tool used to examine the limitations of the capture matrices. Multiple strategies have been employed to investigate the lack of efficient capture: including sample volume, sample introduction and sample speed (36). More efficient target capture by capture matrices could lead to enhanced sensitivity by the immunoassay. These results indicated that when HSA and PG were used to uniformly orient the capture antibody the capture efficiency was improved.

Contaminated food samples were added to the study to test the capabilities of the alternative capture matrix. Ground beef and spinach leaves were tested to determine if these food samples contained components that would interfere with the capture matrix. The supernatant of homogenized ground beef was tested by RAPTOR analysis. Figures 15 and 16 show the limit of detection of *E. coli* O157:H7 was 5.4 x 10^5 CFU/ml for the HSA-PG capture matrix, when homogenized beef and spinach supernatants were tested. The minimal baseline values produced by the biosensor (Appendix B) suggested that components in the beef supernatant did not interfere with the PG in the capture matrix. In contrast, baseline values produced by the biosensor for the spinach supernatant were extremely high (Appendix B). The inherent fluorescence from the chlorophyll (10), in spinach supernatants, could have enhanced the detection by the biosensor; which resulted in false SALOD values and high background noise. The presence of chlorophyll in a food

product is important to consider when fluorescence-based assays are used to detect contamination.

Figure 15 shows the limit of detection for the streptavidin-biotin capture matrix was 5.4 x 10^6 CFU/ml of *E. coli* O157:H7 in ground beef supernatant. For both capture matrices the limit of detection in the ground beef supernatant was less sensitive when compared to limit of detection in PBS (Figure 14). This decrease in sensitivity may be caused by unknown components in the food sample. Large fat or protein particles in the beef supernatant may block antigen binding sites on the waveguide surface, which may have led to decreased sensitivity of the assay (6). Figure 15 shows greater sensitivity by the HSA-PG matrix when compared to streptavidin-biotin in ground beef supernatant. The difference in limits of detection between the capture matrices could be explained by the uniform orientation of the antibodies by HSA-PG, and the random orientation of antibodies by the streptavidin-biotin capture matrix. Uniform antibody orientation has previously shown greater antibody activity when compared to random orientation (24, 40).

An alternative fluorophore was tested for enhanced sensitivity in the biosensor assay when the HSA-PG capture matrix was used. According to the manufacturer, Pierce Biotechnology (Rockford, IL), the DyLight™649 fluorophore is more photo-stable, and produces more intense fluorescence when compared to the Cy5 fluorophore. Figure 19 shows the detection fluorophores did not produce significantly ($P < 0.05$) different SALOD values. These results suggested that the alternative fluorophore failed to enhance the sensitivity of the RAPTOR assay.

Precision was used to measure the reproducibility of the RAPTOR assay, which was a critical characteristic for the immunoassay. Many parameters could diminish precision, e.g., approaching the detection limit of the assay. According to the manufacturer, Research International (Monroe, WA), the detection limits of RAPTOR assays vary depending on the nature of the target. Detection limits are lower for bacterial toxins (0.1 ng/ml to 1,000 ng/ml), as compared to whole bacterial cells (30 CFU/ml to 1.0 x 10^7 CFU/ml). In this study the detection limits of *E. coli* O157:H7 were compared to the precision of the assay. Table 13 shows a total of 136 samples that were assayed using the RAPTOR biosensor, to compare the capture of *E. coli* O157:H7 by streptavidin-biotin and HSA-PG. The precision of both capture matrices was nearly identical, with the exception of 1.0 x 10^2 CFU/ml. The precision of detection, at and below 1.0 x 10^3 CFU/ml of the target bacteria, was below 100%. This decrease in precision indicated that the limit of detection was surpassed, and that the results of the assay were not reliable for sample concentrations below 1.0 x 10^3CFU/ml. Typically, 100% precision or reproducibility would be expected from an immunoassay when the health and safety of consumers is a priority.

Table 13 shows the analysis of a total of 60 RAPTOR waveguides, which were performed to detect *E. coli* O157:H7 or GFP-*E. coli* O157:H7 in PBS. Nine waveguides treated with the streptavidin-biotin capture matrix produced highly variable (CoV > 10%) baseline values. HSA-PG treated waveguides were less variable, with only seven waveguides producing highly variable baseline values. As described in the Materials and Methods section, the data produced by a waveguide with a highly variable baseline was discarded and was not used for graph construction. Baseline variability could be caused

by many factors, including a bowed waveguide (< 180º) or a waveguide that was longer or shorter than 38mm, which were perhaps limitations of the manufacturing process. Figures 14 through 19 did not include data produced by waveguides with a baseline CoV greater than ten percent. Table 13 shows all the waveguides despite the baseline variability.

E. coli CFU/ml	HSA-PG Positive/Negative	Assay Precision	Streptavidin-Biotin Positive/Negative	Assay Precision
10^1	0/2	0%	0/2	0%
10^2	3/9	25%	1/11	8%
10^3	8/6	57%	8/6	57%
10^4	10/0	100%	10/0	100%
10^5	6/0	100%	6/0	100%
10^6	12/0	100%	12/0	100%
10^7	6/0	100%	6/0	100%
10^8	6/0	100%	6/0	100%

TABLE 13. Precision of Capture Matrices

In conclusion, the alternative capture matrix consisted of a 2 to 1 ratio of human serum albumin and streptococcal PG, which immobilized rabbit and goat antibody in a uniform orientation and captured targeted antigen. This uniform antibody orientation led to significantly improved capture efficiency of *E. coli* O157:H7. Further study is required to improve reliable detection below 1.0 x 10^4 CFU/ml for the RAPTOR biosensor.

REFERENCES

1. **Akerstrom, B. and L. Björck.** 1986. A physiochemical study of Protein G, a molecule with unique immunoglobulin G-binding proteins. J. Biol. Chem. **261**:10240-10247.
2. **Åkesson, P., K. Schmidt, J. Cooney and L. Björck.** 1994. M1 protein and protein H: IgGFc- and albumin-binding streptococcal surface proteins encoded by adjacent genes. J. Biochem. **300**:877-886.
3. **Bae, Y. M., B. Oh, W. Lee, W. H. Lee and J. Choi.** 2005. Study on orientation of immunoglobulin G on Protein G layer. Biosensors and Bioelectronics **21**:103-110.
4. **Bjork, L and G. Kronvall**. 1984. Purification and some properties of streptococcal Protein G, a novel IgG-binding reagent. J. Immunol. **133**:969-974.
5. **Crowther, J. R.** 1995. ELISA theory and practice. Methods in molecular biology. **42**:76-77. Humana Press. Totowa, NJ.
6. **DeMarco, D., E. Saaski, D. McCrae and D. V. Lim.** 1999. Rapid detection of *Escherichia coli* O157:H7 in ground beef using a fiber-optic biosensor. J. Food Protection **62**:711-716.
7. **Derrick, J. P. and D. B. Wigley.** 1994. The third IgG-binding domain from streptococcal PG. J. Mol. Biol. **243**:906-918.
8. **Dugaiczyk, A., S. W. Law and O. E. Dennison.** 1982. Nucleotide sequence and the encoded amino acids of human serum albumin mRNA. Proc. Nat. Acad. Sci. **79**:71-75.

9. **Fahenstock, S., Alexander, P., Nagle, J. and Filpula, D.** 1986. Gene for an immunoglobulin binding protein from a group G streptococcus. J. Bacteriol. **167**:870-880.
10. **Frense, D., A. Muller and D. Beckmann.** 1998. Detection of environmental pollutants using optical biosensor with immobilized algae cells. Sensors and Actuators. **51**:256-260.
11. **Golden, J. P., L. Shriver-Lake, G. Anderson, R. Thompson and F. Ligler.** 1992. Fluorometer and tapered fiber optic probes for sensing in the evanescent wave. Optical Engineering. **31**:1458-1462.
12. **GraphPad Software Inc.** 1998. GraphPad InStat version 3.00. Graphpad Software Inc. San Diego, CA.
13. **Green, N. M.** 1990. Avidin and streptavidin. Methods Enzymol. **184**:51-67.
14. **Guss, B., M. Eliasson, A. Olsson, M. Uhlen, A. Frej, H. Jornvall, J. Flock and M. Lindberg.** 1986. Structure of the IgG-binding regions of streptococcal Protein G. EMBO. **5**:1567-1575.
15. **Hirschfeld, T. E.** May 1984. Fluorescent immunoassay employing optical fiber in capillary tube. U.S. patent 4,447,546.
16. **Hnatowich, D. J., F. Virizi and M. Rusckowski.** 1987. Investigations of avidin and biotin for imaging applications. J. Nucl. Med. **28**:1294-1302.
17. **Johansson, M., I. Frick, H. Nilsson, P. Kraulis, S. Hober, P. Jonasson, M. Linhult, P. Nygren, M. Uhlén, L. Björck, T. Drakenberg, S. Forsén and M. Wikström.** 2002. Structure, specificity, and mode of interaction for bacterial albumin-binding modules. J. Biol. Chem. **277**:8114-8120.

18. **Konig, T. and A. Skerra.** 1998. Use of an albumin-binding domain for the selective immobilization of recombinant capture antibody fragments on ELISA plates. J. Immun. Methods **218**:73-83.

19. **Kramer, M. F. and D. V. Lim.** 2004. A rapid and automated fiber optic-based biosensor assay for the detection of Salmonella in spent irrigation water used in the sprouting of sprout seeds. J. Food Protection **67**:46-52.

20. **Kraulis, P., P. Jonasson, P. Nygren, M. Uhlén, L. Jendedberg, B. Nilsson and J. Kördel.** 1996. The serum albumin-binding domain of streptococcal protein G is a three-helical bundle: a heteronuclear NMR study. FEBS Letters. **378**:190-194.

21. **Kronvall, G.** 1973. A surface componenet in group A, C and G streptococci with non-immune reactivity for immunoglobulin G. J. Immunol. **111**:1401-1406.

22. **Laitinen, O., H. Nordlund, V. Hytonen, and M. Kolumaa.** 2007. Brave new (strept)avidins in biotechnology. Trends Biotech. **25**:269-277.

23. **Leskinen, S. D. and D. V. Lim.** 2008. Rapid ultrafiltration concentration and biosensor detection of enterococci from large volumes of Florida recreational water. Appl. Environ. Microbiol. **74**:4792-4798.

24. **Lu, B., M. Smyth and R. O'Kennedy.** 1996. Oriented immobilization of antibodies and its applications in immunoassays and immunosensors. Analyst. **121**:29R-32R.

25. **Myhre, E. and G. Kronvall.** 1977. Heterogeneity of nonimmune immunoglobulin Fc reactivity among Gram-positive cocci: Description of three major types of receptors for human immunoglobulin G. Infection and Immun. **17**:475-482.

26. **Nanninga, N.** 1998. Morphogenesis of *Escherichia coli.* Micro. Mol. Bio. Reviews. **62**:110-129.

27. **Nitsche-Schmitz, D. P., H. M. Johansson, I. Sastalla, S. Reissmann, I. Frick and G. S. Chhatwal.** 2007. Group G streptococcal IgG binding molecules FOG and Protein G have different impacts on opsonization by C1q. J. Bio. Chem. **202**:17530-17536.

28. **Nygren, P., M. Eliassson, L. Abrahmsén and M. Uhlén.** 1988. Analysis and use of the serum albumin binding domains of streptococcal protein G. J. Mol. Recog. **1**:69-74.

29. **Nygren, P., C. Ljungquist, H. Trømborg. K Nustad and M. Uhlén.** 1990 Species-dependent binding of serum albumins to the streptococcal protein G. Eur. J. Biochem. **193**:143-148.

30. **Olsson, A., M. Eliasson, B. Guss, B. Nilsson, U. Hellman, M. Lindberg and M. Uhlén.** 1987. Structure and evolution of the repetitive gene encoding streptococcal protein G. Eur. J. Biochem. **168**:319-324.

31. **Peluso, P., D. S. Wilson, D. Do, H. Tran, M. Venkatasubbaiah, D. Quincy, B. Heidecker, K. Poindexter, N. Tolani, M. Phelan, K. Witte, L. S. Jung, P. Wanger and S. Nock.** 2003. Optimizing antibody immobilization strategies for the construction of protein microarrays. Anal. Biochem. **312**:113–124.

32. **Reis, K., E. Ayoub and M. Boyle.** 1984. Streptococcal Fc receptors I. Isolation and partial characterization of the receptor for a Group C streptococcus. J. Immunol. **132**:3091-3097.

33. **Reis, K., E. Ayoub and M. Boyle.** 1984. Streptococcal Fc receptors II. Comparison of the reactivity of a receptor from a group C streptococcus with staphylococcal protein A. J. Immunol. **132**:3098-3102.

34. **Shriver-Lake, L., B. Donner, R. Edelstein, K. Breslin, S. K. Bhatia and F. S. Ligler.** 1997. Antibody immobilization using heterobifunctional crosslinkers. Biosensors and Bioelectronics **12**:1101-1106.

35. **Shriver-Lake, L., S. Turner and C. R. Taitt.** 2007. Rapid detection of *E. coli* O157:H7 spiked into food matrices. Analy. Chim. Acta. **584**:66-71.

36. **Simpson-Stroot, J., E. Kearns, P. Stroot, S. Magana and D. V. Lim.** 2008. Monitoring biosensor capture efficiencies: Development of a model using GFP-expressing *Escherichia coli* O157:H7. J. Mircro. Methods **72**:29-37.

37. **Sjöbring, U., C. Falkenberg, E. Nielsen, B. Åkerström and L. Björck.** 1988. Isolation and characterization of a 14-kDa albumin-binding fragment of streptococcal protein G. J. Immunol. **140**:1595-1599.

38. **Sugio, S., A. Kashima, S. Mochizuki, M. Noda and K. Kobayashi.** 1999. Crystal structure of human serum albumin at 2.5Å resolution. Prot. Engin. **12**:439-446.

39. **Suter, M., J. E. Butler and J. H. Peterman.** 1989. The immunochemistry of sandwich ELISAs-III. The stoichiometry and efficacy of the protein-avidin-biotin capture (PABC) system. Mol. Immun. **23**:221-230.

40. **Vijayendran, R. and D. Leckband.** 2001. A quantitative assessment of heterogeneity for surface-immobilized proteins. Anal. Chem. **73**:471-480.

APPENDICES

Appendix A: ELISA Analysis

TABLE 14. Functional Albumin Binding Domain, HSA Role in Capture Matrix

	HSA in Columns (µg/ml)											
	0.0	0.0	0.5	0.5	1.0	1.0	0.0	0.0	0.5	0.5	1.0	1.0
0.0 µg/ml PG	121.5	125.7	120.1	130.7	138.3	131.5	**151.8**	**129.5**	**140.3**	**140.7**	**134.4**	**130.4**
0.25 µg/ml PG	121.2	134.2	967.9	1044.4	1545.5	1569.1	**160.5**	**131.7**	**138.3**	**140.7**	**134.5**	**130.5**
0.5 µg/ml PG	132.2	127.1	1172.5	1231.9	1848.1	1864.9	**138.2**	**125.3**	**131.7**	**131.5**	**134.0**	**133.2**
1.0 µg/ml PG	119.8	130.1	1216.3	1344.5	1943.5	1907.6	**136.9**	**123.3**	**133.4**	**143.7**	**128.9**	**129.7**
2.5 µg/ml PG	122.5	134.2	1380.9	1336.1	1991.1	1997.7	**141.1**	**136.8**	**132.5**	**138.1**	**132.2**	**132.6**
5.0 µg/ml PG	110.7	153.9	1555.3	1518.7	2147.5	2132.7	**138.5**	**120.8**	**127.3**	**128.1**	**132.0**	**126.0**
10.0 µg/ml PG	117.1	148.8	1605.5	1570.8	2212.6	2140.0	**158.1**	**136.9**	**136.6**	**139.2**	**134.8**	**137.7**
20.0 µg/ml PG	139.2	157.5	1583.2	1567.1	2180.5	2222.2	**142.6**	**135.6**	**147.9**	**133.7**	**139.5**	**137.3**
0.0 µg/ml PG	148.7	168.1	158.5	158.6	151.4	156.8	**185.8**	**170.3**	**169.2**	**173.6**	**163.6**	**144.0**
0.25 µg/ml PG	139.8	180.0	985.0	997.9	1488.4	1485.6	**221.3**	**197.3**	**166.1**	**186.1**	**147.3**	**150.1**
0.5 µg/ml PG	153.2	176.0	1565.4	1372.8	2207.2	2119.1	**205.8**	**156.8**	**141.0**	**173.5**	**141.4**	**138.5**
1.0 µg/ml PG	153.6	157.8	1362.4	1650.2	2038.4	2318.9	**257.4**	**163.2**	**143.3**	**154.9**	**150.5**	**139.9**
2.5 µg/ml PG	125.4	160.4	1343.0	1335.4	1666.3	1891.0	**148.7**	**158.8**	**141.6**	**149.8**	**139.2**	**155.1**
5.0 µg/ml PG	119.9	135.4	1270.4	1267.8	1750.9	1763.3	**137.6**	**133.7**	**131.9**	**126.4**	**138.6**	**135.8**
10.0 µg/ml PG	127.0	176.0	1284.0	1294.7	1741.9	1715.2	**143.7**	**137.4**	**126.4**	**120.7**	**129.0**	**127.4**
20.0 µg/ml PG	148.1	169.6	1264.1	1255.6	1609.3	1641.3	**140.1**	**143.4**	**145.3**	**140.7**	**137.4**	**139.5**
0.0 µg/ml PG	134.6	150.6	146.2	148.4	144.2	150.1	**160.8**	**162.6**	**166.4**	**167.8**	**153.8**	**159.1**
0.25 µg/ml PG	144.6	157.2	1054.0	1144.2	1751.6	1788.0	**171.6**	**174.2**	**164.6**	**171.0**	**147.9**	**168.1**
0.5 µg/ml PG	150.9	176.1	1698.5	1698.2	2433.0	2393.8	**159.9**	**162.0**	**142.1**	**152.1**	**138.2**	**147.4**
1.0 µg/ml PG	135.3	161.5	1257.5	1348.0	2045.4	2037.5	**155.7**	**171.5**	**146.8**	**143.8**	**141.8**	**158.3**
2.5 µg/ml PG	137.1	170.5	1599.6	1573.7	2423.7	2467.9	**168.3**	**165.8**	**162.2**	**155.5**	**144.3**	**134.8**
5.0 µg/ml PG	112.7	137.0	1125.0	1046.9	1910.6	2060.7	**127.5**	**129.4**	**130.1**	**131.8**	**134.2**	**123.1**
10.0 µg/ml PG	133.7	203.2	1107.9	1107.0	1542.3	1569.7	**143.6**	**147.4**	**133.1**	**142.1**	**134.7**	**133.3**
20.0 µg/ml PG	139.2	146.7	1024.8	1119.4	1533.8	1590.1	**140.5**	**144.8**	**141.5**	**147.2**	**141.8**	**141.2**

No Bold Indicates Native PG **Bold Indicates Recombinant PG**

TABLE 15. Alternative Albumin Species

	Albumin in columns (µg/ml)											
	1 OVA	1 OVA	5 OVA	5 OVA	1 BSA	1 BSA	5 BSA	5 BSA	1 HSA	1 HSA	5 HSA	5 HSA
0 µg/ml PG	283.9	206.0	187.9	185.4	258.7	279.2	188.8	217.8	253.0	261.4	173.7	215.6
0.25 µg/ml PG	318.6	273.7	185.2	182.3	303.0	291.8	327.4	354.0	2615.2	2601.9	2781.5	2889.5
0.5 µg/ml PG	289.4	255.1	186.9	187.3	320.5	319.2	453.2	383.0	3056.6	3079.6	3245.5	3389.8
1 µg/ml PG	317.2	285.3	186.1	188.6	382.3	357.4	549.1	591.0	3269.9	3368.2	3524.3	3692.3
2.5 µg/ml PG	224.1	272.1	197.0	192.5	434.5	465.4	705.6	709.1	3353.6	3380.7	3959.2	3934.0
5 µg/ml PG	237.0	348.8	245.5	211.4	466.3	488.8	915.1	864.9	3381.7	3363.5	3903.6	3926.4
No PG	181.3	244.7	244.9	154.1	258.3	254.2	250.6	242.7	300.4	258.0	209.7	234.9
	PG in columns (µg/ml)											
	0.0	0.0	0.25	0.25	0.5	0.5	1.0	1.0	2.5	2.5	5.0	5.0
No Albumin	341.4	432.3	552.3	639.8	754.2	804.2	838.9	1227.0	1375.8	1471.7	1786.3	1869.4
	Albumin in columns (µg/ml)											
	1 OVA	1 OVA	5 OVA	5 OVA	1 BSA	1 BSA	5 BSA	5 BSA	1 HSA	1 HSA	5 HSA	5 HSA
0 µg/ml PG	256.7	287.9	221.5	272.7	278.7	266.1	182.9	258.9	269.6	288.0	236.2	240.5
0.25 µg/ml PG	264.6	322.7	279.8	261.3	353.2	327.8	343.6	312.2	2745.5	2732.9	3043.3	3024.1
0.5 µg/ml PG	287.2	282.1	304.9	293.8	348.7	344.1	543.2	383.0	3188.7	3121.8	3413.9	3413.0
1 µg/ml PG	318.5	360.6	304.3	290.1	391.4	382.9	594.5	531.2	3447.2	3552.8	3670.1	3761.8
2.5 µg/ml PG	292.8	342.3	333.6	262.4	447.7	469.9	763.7	748.4	3471.6	3482.8	3856.7	3975.0
5 µg/ml PG	292.4	367.4	338.5	327.7	503.3	564.2	870.9	892.0	3460.0	3442.9	3847.0	3935.9
No PG	261.3	221.0	277.4	210.3	278.3	269.9	206.2	216.6	305.6	242.2	228.9	255.8
	PG in columns (µg/ml)											
	0.0	0.0	0.25	0.25	0.5	0.5	1.0	1.0	2.5	2.5	5.0	5.0
No Albumin	482.5	575.4	882.6	637.6	796.7	900.8	825.1	1086.6	1536.8	1445.1	1753.2	2252.4

TABLE 15. Alternative Albumin Species (Continued)

	Albumin in columns (µg/ml)											
	1 OVA	1 OVA	5 OVA	5 OVA	1 BSA	1 BSA	5 BSA	5 BSA	1 HSA	1 HSA	5 HSA	5 HSA
0 µg/ml PG	243.6	278.9	285.8	264.6	294.2	370.9	291.9	285.1	291.8	351.8	263.4	294.8
0.25 µg/ml PG	280.6	322.8	270.6	269.1	383.2	418.3	388.5	395.1	3122.7	3117.1	3304.2	3608.9
0.5 µg/ml PG	356.0	277.9	290.6	277.9	499.7	348.5	438.5	476.3	3569.9	3534.5	3695.1	3447.3
1 µg/ml PG	417.7	313.3	313.4	370.2	454.9	366.0	587.4	576.9	3669.6	3775.5	4012.5	4225.8
2.5 µg/ml PG	313.5	376.7	385.7	329.1	490.8	478.9	753.2	764.0	3733.5	3753.3	4010.9	4091.0
5 µg/ml PG	332.0	360.2	405.2	473.7	648.5	598.2	931.7	999.6	3681.5	3771.9	3870.9	3870.8
No PG	209.2	265.1	276.0	216.5	309.1	272.3	248.0	235.6	247.3	313.8	261.9	245.5
	PG in columns (µg/ml)											
	0.0	0.0	0.25	0.25	0.5	0.5	1.0	1.0	2.5	2.5	5.0	5.0
No Albumin	490.6	717.7	739.0	1021.0	825.1	798.4	1214.2	929.5	1129.4	1123.8	909.7	1119.3

TABLE 16. HSA Role in Capturing Bacteria

	PG in Columns (µg/ml)											
	0.0	0.0	0.25	0.25	0.5	0.5	1.0	1.0	2.5	2.5	5.0	5.0
No Bacteria	142.4	156.4	162.0	179.6	176.5	187.7	174.2	182.0	174.7	181.7	197.5	190.9
4.70E+07	1524.2	1239.7	2741.1	2778.8	2924.7	2810.5	2883.3	2866.0	2855.7	2792.6	2844.2	2856.5
4.70E+06	449.9	373.1	2431.2	2563.4	2551.7	2630.7	2814.7	2529.5	2835.8	2845.2	2797.3	2862.5
4.70E+05	165.0	155.6	1599.6	1755.5	1877.2	2027.4	2201.0	2081.7	2235.8	2217.2	2288.3	2310.1
4.70E+04	136.8	134.7	1287.0	1284.8	1476.1	1643.3	1888.5	1733.4	1817.3	1766.8	1961.6	1979.6
4.70E+03	119.9	116.0	1015.0	1156.6	1273.9	1393.9	1617.6	1503.8	1742.0	1628.1	1691.9	1842.3
4.70E+02	112.7	112.1	951.1	1023.7	1337.4	1292.5	1408.8	1419.4	1443.9	1481.4	1512.5	1540.9
4.70E+01	105.3	115.8	799.9	930.8	1279.1	1235.3	1349.6	1339.6	1434.8	1401.5	1473.9	1500.4
No Bacteria	145.5	146.4	175.5	184.3	178.6	185.7	169.1	175.4	179.3	180.7	197.5	193.0
4.70E+07	1344.2	1264.4	3102.7	3152.6	3280.2	3240.1	3270.6	3266.1	3218.9	3233.4	3192.5	3189.9
4.70E+06	392.8	303.0	3150.1	3066.3	3102.6	2839.1	2830.7	3002.7	2935.2	2937.8	3159.7	3173.7
4.70E+05	154.5	138.6	2039.2	2100.1	2151.4	2208.6	2240.3	2365.5	2350.2	2427.0	2479.2	2448.0
4.70E+04	141.2	125.4	1859.5	1859.3	2029.2	1980.4	2133.2	2192.6	2286.9	2182.5	2329.6	2367.2
4.70E+03	116.8	123.3	1730.8	1673.5	1863.0	1862.2	2145.3	1963.9	2233.5	2336.7	2165.5	2363.7
4.70E+02	123.0	108.7	1509.9	1524.9	1695.3	1636.0	1884.6	1764.5	1890.9	1928.5	1904.5	2009.8
4.70E+01	111.9	123.1	1475.3	1475.7	1706.6	1668.9	1772.1	1813.6	1815.0	1848.4	1916.0	1965.5
No Bacteria	133.6	156.3	146.7	158.6	152.2	160.2	162.1	169.6	190.7	201.8	189.5	194.7
4.70E+07	1343.1	1064.5	3012.3	3162.5	3290.1	3244.0	3267.6	3265.0	3154.1	3238.5	3162.3	3191.9
4.70E+06	370.5	279.4	2824.8	2843.5	2911.1	3040.8	3050.0	3155.0	3311.8	3112.6	3135.1	3105.0
4.70E+05	177.6	137.2	2188.7	2128.9	2267.7	2262.9	2380.5	2481.7	2613.2	2480.9	2444.5	2382.7
4.70E+04	124.1	126.4	1816.6	1825.3	2032.3	2010.3	1990.0	2026.3	2123.8	1911.4	1939.7	1772.2
4.70E+03	118.6	113.5	1699.6	1849.7	1917.4	1836.0	1792.6	1787.7	1884.6	1773.5	1830.1	1738.4
4.70E+02	119.1	119.7	1660.8	1658.0	1791.3	1603.7	1709.5	1702.6	1881.5	1768.6	1758.6	1726.1
4.70E+01	114.5	129.9	1610.2	1463.8	1642.9	1615.4	1757.3	1702.0	1779.4	1737.2	1678.0	1651.2

E. coli O157:H7 in Rows (CFU/ml)

TABLE 17. Optimal Ratio of HSA to PG

	PG in columns (µg/ml)											
	0.0	0.5	1.0	2.5	5.0	10.0	0.0	0.5	1.0	2.5	5.0	10.0
0 µg/ml HSA	1746.1	3675.8	5101.3	5678.2	5961.1	6329.3	**354.8**	**399.8**	**723.4**	**403.2**	**557.5**	**760.0**
0 µg/ml HSA	2823.3	3974.7	5264.7	5754.9	5948.0	6246.4	**326.2**	**433.7**	**456.9**	**430.9**	**550.5**	**622.3**
	HSA in columns (µg/ml)											
	1.0	1.0	5.0	5.0	10.0	10.0	1.0	1.0	5.0	5.0	10.0	10.0
0.0 µg/ml PG	1124.8	1026.1	968.0	1050.0	1070.1	1056.1	**114.7**	**103.6**	**111.1**	**119.9**	**156.2**	**127.9**
0.5 µg/ml PG	6233.9	6542.3	6769.8	6716.6	6725.1	6490.1	**402.6**	**401.8**	**585.5**	**625.8**	**634.9**	**656.0**
1.0 µg/ml PG	6309.1	6267.5	6723.4	6504.4	6702.4	6499.8	**437.9**	**462.8**	**740.7**	**741.0**	**765.1**	**875.4**
2.5 µg/ml PG	6187.0	6294.2	6578.0	6400.9	6549.4	6304.0	**641.8**	**654.6**	**849.3**	**863.3**	**967.5**	**1007.4**
5.0 µg/ml PG	6102.8	6207.8	6581.1	6433.4	6511.9	6461.5	**607.5**	**625.1**	**857.6**	**882.3**	**962.2**	**1012.7**
10.0 µg/ml PG	6123.5	6386.5	6562.1	6527.9	6574.4	6597.5	**717.8**	**745.0**	**1035.6**	**994.8**	**1106.9**	**1147.5**

No Bold Indicates 8.1×10^7 CFU/ml *E. coli* O157:H7 **Bold indicates no bacteria**

TABLE 18. Species Specific Fc Binding Domain

	PG in Columns (µg/ml)					
	0.0	0.0	0.5	0.5	1.0	1.0
0 µg/ml IgG	**90.1**	**95.2**	**93.5**	**92.6**	**94.5**	**97.3**
0.25 µg/ml IgG	**92.9**	**92.2**	**692.9**	**693.9**	**643.1**	**672.2**
0.5 µg/ml IgG	**97.4**	**94.6**	**994.8**	**993.2**	**1387.0**	**1402.0**
1.0 µg/ml IgG	**93.3**	**91.4**	**1391.8**	**1407.7**	**1499.2**	**1501.3**
0 µg/ml IgG	92.0	88.3	90.6	92.7	89.2	91.1
0.25 µg/ml IgG	99.5	84.5	88.7	88.3	88.1	92.8
0.5 µg/ml IgG	90.3	85.7	88.2	88.7	88.9	89.9
1.0 µg/ml IgG	88.1	88.1	89.0	87.1	89.6	91.9
0 µg/ml IgG	**88.4**	**90.2**	**89.4**	**89.0**	**91.1**	**95.6**
0.25 µg/ml IgG	**93.2**	**98.0**	**602.2**	**593.8**	**653.1**	**772.2**
0.5 µg/ml IgG	**94.7**	**90.5**	**1394.8**	**1393.1**	**1388.1**	**1472.0**
1.0 µg/ml IgG	**98.5**	**95.9**	**1491.8**	**1411.8**	**1497.5**	**1521.4**
0 µg/ml IgG	88.1	85.9	88.8	89.6	87.4	88.6
0.25 µg/ml IgG	90.2	93.4	92.1	91.6	94.0	103.1
0.5 µg/ml IgG	96.5	91.7	88.8	88.1	81.6	85.2
1.0 µg/ml IgG	94.0	93.2	96.1	93.1	94.4	91.1
0 µg/ml IgG	**94.3**	**95.3**	**93.4**	**93.8**	**94.4**	**100.5**
0.25 µg/ml IgG	**91.8**	**98.6**	**640.3**	**632.2**	**646.0**	**631.8**
0.5 µg/ml IgG	**100.5**	**109.8**	**1181.0**	**1192.3**	**1088.2**	**1085.0**
1.0 µg/ml IgG	**103.2**	**119.7**	**1372.3**	**1304.4**	**1367.0**	**1313.2**
0 µg/ml IgG	97.6	91.5	92.7	89.4	90.6	93.9
0.25 µg/ml IgG	130.5	111.4	105.7	109.0	104.6	101.8
0.5 µg/ml IgG	108.0	112.4	100.7	112.4	102.4	119.3
1.0 µg/ml IgG	109.9	101.6	134.9	112.3	102.9	103.6

Bold Indicates HRP goat anti- rabbit and mouse anti- *E. coli* O157:H7
No Bold Indicates HRP mouse anti- rabbit and goat anti- *E. coli* O157:H7

TABLE 19. Optimal Capture Antibody Species

	HSA in Columns (µg/ml)											
	0.0	0.0	0.5	0.5	1.0	1.0	0.0	0.0	0.5	0.5	1.0	1.0
0.0 µg/ml PG	93.3	95.6	111.9	109.5	124.8	107.4	*132.8*	*137.8*	*115.9*	*113.5*	*121.2*	*106.6*
0.5 µg/ml PG	108.7	103.1	340.6	334.8	603.5	672.0	*152.2*	*147.5*	*523.6*	*552.9*	*819.1*	*810.1*
1.0 µg/ml PG	117.3	131.2	397.0	405.0	738.5	742.9	*149.6*	*143.9*	*940.7*	*945.8*	*921.1*	*1011.2*
2.5 µg/ml PG	107.7	107.2	446.4	489.4	849.5	904.5	*193.1*	*212.0*	*1014.7*	*989.6*	*1156.7*	*1488.4*
0.0 µg/ml PG	**119.1**	**101.9**	**105.1**	**111.3**	**121.8**	**134.7**	***166.8***	***182.7***	***139.8***	***159.5***	***140.8***	***143.8***
0.5 µg/ml PG	**126.8**	**116.9**	**116.5**	**129.5**	**109.6**	**114.0**	***157.3***	***157.8***	***145.1***	***162.7***	***145.1***	***146.4***
1.0 µg/ml PG	**109.7**	**129.7**	**112.8**	**114.3**	**146.0**	**111.5**	***207.6***	***169.8***	***136.5***	***160.8***	***154.2***	***164.0***
2.5 µg/ml PG	**125.9**	**114.2**	**127.7**	**125.7**	**130.6**	**137.8**	***171.8***	***155.5***	***163.3***	***168.2***	***156.6***	***156.7***
0.0 µg/ml PG	120.3	105.9	92.6	120.0	131.5	119.2	*128.8*	*146.3*	*117.4*	*106.5*	*126.0*	*114.7*
0.5 µg/ml PG	108.6	112.1	464.3	476.3	886.2	828.7	*166.5*	*164.4*	*586.1*	*564.0*	*996.1*	*970.9*
1.0 µg/ml PG	112.8	109.4	657.7	659.8	1030.4	910.4	*142.4*	*145.9*	*671.1*	*674.9*	*1163.3*	*1439.9*
2.5 µg/ml PG	124.3	136.7	644.6	712.9	1293.0	1117.3	*183.0*	*134.8*	*712.3*	*848.9*	*1344.3*	*1502.8*
0.0 µg/ml PG	**105.8**	**134.3**	**93.4**	**102.0**	**135.9**	**118.2**	***210.4***	***128.2***	***115.3***	***126.6***	***139.3***	***129.9***
0.5 µg/ml PG	**93.0**	**105.8**	**109.0**	**119.7**	**113.1**	**131.9**	***185.3***	***143.4***	***125.6***	***131.5***	***128.4***	***134.1***
1.0 µg/ml PG	**91.6**	**101.0**	**115.8**	**132.4**	**93.2**	**104.9**	***247.1***	***193.9***	***124.6***	***143.7***	***130.2***	***152.2***
2.5 µg/ml PG	**113.0**	**106.1**	**118.0**	**130.7**	**140.5**	**152.4**	***192.9***	***207.9***	***172.5***	***167.6***	***152.2***	***170.4***
0.0 µg/ml PG	104.1	118.4	99.4	365.8	93.2	110.5	*137.2*	*163.3*	*121.7*	*119.2*	*111.5*	*117.9*
0.5 µg/ml PG	106.3	115.8	395.9	410.1	785.3	812.8	*171.1*	*172.2*	*527.4*	*528.2*	*1021.4*	*995.6*
1.0 µg/ml PG	111.6	98.7	510.2	462.6	939.2	937.2	*135.8*	*166.9*	*647.4*	*663.1*	*1136.6*	*1411.8*
2.5 µg/ml PG	97.7	135.1	593.7	555.3	1019.4	1047.1	*174.8*	*159.8*	*787.3*	*859.9*	*1342.5*	*1703.2*
0.0 µg/ml PG	**129.7**	**103.5**	**129.1**	**101.4**	**101.7**	**101.1**	***189.0***	***154.3***	***125.9***	***134.5***	***140.2***	***149.5***
0.5 µg/ml PG	**120.4**	**115.2**	**114.5**	**126.3**	**147.4**	**171.0**	***197.3***	***148.0***	***137.6***	***123.3***	***149.7***	***146.3***
1.0 µg/ml PG	**110.7**	**109.9**	**130.1**	**118.2**	**103.7**	**101.8**	***204.2***	***227.6***	***151.7***	***150.7***	***140.5***	***152.2***
2.5 µg/ml PG	**97.0**	**119.0**	**132.9**	**121.6**	**122.5**	**153.8**	***213.5***	***212.1***	***176.1***	***165.2***	***164.3***	***169.0***

Bold indicates PG lacking ABD
No Bold Indicates Rabbit anti- Goat and Mouse anti- Rabbit
Italics indicate Goat anti- E. coli O157:H7 and Mouse anti- Goat

TABLE 20. Optimal Concentration of Detector Antibody

HRP goat anti E. coli O157:H7 in Columns (µg/ml)

	1.0	1.0	2.5	2.5	5.0	5.0
3.0E+08	7454.3	8396.7	8158.9	7386.7	7414.3	7830.8
3.0E+07	7246.4	7924.8	7819.1	7454.5	7467.1	7337.9
3.0E+06	5887.1	6487.0	7122.4	6892.7	7150.1	7117.9
3.0E+05	2113.9	2357.2	3008.6	2865.5	3557.0	3459.8
3.0E+04	1191.3	1318.7	1646.9	1604.3	2147.9	2218.6
3.0E+03	1041.3	1116.6	1526.6	1470.1	2161.9	1979.5
1.5E+07	**1030.2**	**1118.8**	**1530.2**	**1376.5**	**1933.9**	**1862.0**
No Bacteria	1257.1	1372.3	1784.7	1656.7	2229.4	2229.1
3.0E+08	8570.0	8511.2	8420.4	8491.2	8603.5	8335.1
3.0E+07	8326.0	8585.6	8786.3	8824.7	8528.1	8279.8
3.0E+06	7950.3	8187.4	8607.0	8670.4	8747.8	8623.5
3.0E+05	4006.4	4006.6	4842.5	4463.9	5277.0	5029.3
3.0E+04	1768.8	1908.4	2281.1	2288.1	2591.5	2547.3
3.0E+03	1466.3	1495.8	1925.2	1841.8	2446.4	2445.9
1.5E+07	**1437.4**	**1325.7**	**1760.9**	**1727.6**	**2437.2**	**2070.2**
No Bacteria	1478.7	1370.9	1981.0	2128.8	2886.9	2545.5
3.0E+08	6850.5	6956.6	7310.9	7229.6	7441.9	7269.4
3.0E+07	6941.1	7097.3	7393.7	7128.7	7474.1	7365.0
3.0E+06	6699.5	6677.4	7307.0	7054.4	7364.7	7335.9
3.0E+05	3323.8	3247.1	4093.6	4023.1	4741.9	4593.5
3.0E+04	1283.6	1355.0	1667.3	1661.7	2042.7	2041.9
3.0E+03	1092.3	1166.3	1609.7	1656.4	2070.9	2067.4
1.5E+07	**1055.8**	**1103.2**	**1617.1**	**1630.4**	**2064.6**	**2035.6**
No Bacteria	1149.7	1138.0	1828.6	1798.2	2625.5	2697.2

Bold Indicates E. coli K-12 (CFU/ml)

No Bold Indicates E. coli O157:H7 (CFU/ml)

TABLE 21. The Limit of Detection Using ELISA, Capture Antibody Displacement

Concentration of HRP goat anti E. coli O157:H7 (µg/ml)

	0.1	0.1	0.5	0.5	1.0	1.0	0.1	0.1	0.5	0.5	1.0	1.0
No Bacteria	89.6	86.1	155.3	218.5	329.2	297.8	**96.9**	**96.8**	**203.6**	**207.8**	**247.9**	**235.4**
K-12 (6.0x10^6)	85.4	84.4	137.8	150.3	284.6	208.4	**95.5**	**94.0**	**198.5**	**196.7**	**230.9**	**229.1**
O157 (9.7x10^2	81.3	83.6	132.9	154.0	210.4	223.9	**86.1**	**88.0**	**161.9**	**132.7**	**237.2**	**260.4**
O157 (9.7x10^3	96.7	99.4	146.7	182.2	300.3	272.3	**98.6**	**97.7**	**106.8**	**107.9**	**217.4**	**247.5**
O157 (9.7x10^4	321.3	317.1	650.9	773.9	1027.0	1089.0	**349.8**	**317.6**	**605.1**	**617.4**	**1070.9**	**1063.9**
O157 (9.7x10^5	1591.9	1399.8	4494.9	3945.1	5143.7	5388.6	**2534.4**	**2527.4**	**5969.6**	**5451.6**	**6958.3**	**6994.6**
O157 (9.7x10^6	2461.7	2353.1	5819.7	5947.2	7047.7	6940.5	**3737.0**	**3735.9**	**6250.2**	**6274.6**	**7906.0**	**7936.7**
O157 (9.7x10^7	1697.2	1735.8	5084.4	4868.8	6241.9	6216.4	**2396.0**	**2446.9**	**5913.9**	**5884.7**	**6862.2**	**6674.8**
No Bacteria	95.1	96.3	168.1	227.9	356.8	376.5	**81.4**	**80.4**	**166.9**	**212.5**	**264.7**	**326.7**
K-12 (6.0x10^6)	99.1	95.7	142.3	161.5	297.3	261.3	**79.1**	**81.1**	**138.0**	**124.8**	**240.2**	**177.7**
O157 (9.7x10^2	89.0	86.2	141.9	190.0	201.4	354.2	**84.2**	**93.1**	**156.2**	**139.1**	**254.8**	**285.2**
O157 (9.7x10^3	93.7	96.1	131.4	203.1	233.3	334.6	**102.2**	**97.5**	**166.9**	**184.8**	**278.0**	**301.8**
O157 (9.7x10^4	375.1	338.1	620.2	641.4	646.7	688.8	**381.8**	**349.7**	**880.0**	**878.2**	**1181.3**	**1203.4**
O157 (9.7x10^5	1744.9	1706.7	4213.0	4107.0	5188.0	5232.0	**1728.8**	**1625.2**	**4348.3**	**4386.8**	**5607.5**	**5492.9**
O157 (9.7x10^6	2840.1	2781.4	6257.0	6202.9	6861.5	6915.5	**2694.0**	**2536.5**	**6199.0**	**6282.9**	**7092.1**	**6921.8**
O157 (9.7x10^7	2476.7	2472.3	6068.0	5893.2	6985.6	6734.7	**1766.8**	**1792.1**	**5139.6**	**4703.5**	**6232.1**	**6136.6**
No Bacteria	92.2	95.7	269.9	224.8	335.3	376.4	**84.1**	**90.5**	**147.0**	**204.0**	**287.7**	**355.8**
K-12 (6.0x10^6)	90.2	99.5	247.2	244.0	264.1	283.5	**77.4**	**82.9**	**121.2**	**138.7**	**208.5**	**220.2**
O157 (9.7x10^2	99.3	96.8	141.1	118.4	196.3	197.9	**82.2**	**86.5**	**169.9**	**129.0**	**190.6**	**193.8**
O157 (9.7x10^3	92.4	91.8	178.2	147.8	230.2	242.9	**100.2**	**103.8**	**315.2**	**171.0**	**229.6**	**234.6**
O157 (9.7x10^4	367.5	398.5	607.9	629.5	687.3	697.8	**354.9**	**347.9**	**826.1**	**813.3**	**1100.3**	**1146.0**
O157 (9.7x10^5	1827.0	1466.1	4290.3	4267.6	5570.8	5237.6	**1631.9**	**1552.4**	**4268.2**	**4270.9**	**5454.7**	**5417.0**
O157 (9.7x10^6	3017.5	2330.4	6816.9	6480.9	7163.7	7080.6	**2487.6**	**2533.1**	**6255.4**	**6297.5**	**7230.0**	**7237.2**
O157 (9.7x10^7	2706.4	2121.4	6476.5	6352.5	7078.5	6895.3	**1827.7**	**1759.6**	**5241.3**	**5260.0**	**6831.9**	**6892.4**

No Bold Indicates Streptavidin-Biotin-IgG **Bold Indicates HSA-PG-IgG**

Appendix B: RAPTOR Analysis

TABLE 22. The Limit of Detection of Two Capture Matrices Using RAPTOR Analysis

		Strept-Biotin	HSA-PG	HSA-PG	Strept-Biotin
Baseline Signals	Baseline 1	691.9	520.5	535.3	822.1
	Baseline 2	799.2	558.5	645.3	864.2
	Baseline 3	913.2	590.3	747.5	949.9
	Baseline 4	1013.1	622.6	820.8	1115.6
Normalization Coefficients	B1/**LC** = B1N	1.3	1.0	1.0	1.6
	B2/**LC** = B2N	1.4	1.0	1.2	1.5
	B3/**LC** = B3N	1.5	1.0	1.3	1.6
	B4/**LC** = B4N	1.6	1.0	1.3	1.8
Normalized Baselines	B1/ B4N	425.2	520.5	406.0	458.8
	B2/B4N	491.1	558.5	489.5	482.3
	B3/B4N	561.2	590.3	567.0	530.1
	B4/B4N	622.6	622.6	622.6	622.6
	Average	525.0	573.0	521.3	523.5
	STDEV	85.5	43.7	94.2	72.5
	%CoV	16.3	7.6	18.1	13.8
E. coli O157:H7 Signals	10^-6	1139.7	651.9	917.3	1169.5
	10^-5	1228.2	685.2	965.9	1303.5
	10^-4	1357.3	728.3	1099.6	1333.7
Normalized Ec Signals	10^-6/B4N	700.4	651.9	695.8	652.7
	10^-5/B4N	754.8	685.2	732.7	727.5
	10^-4/B4N	834.1	728.3	834.1	744.3
Limit of Detection	LOD	781.6	704.0	804.0	740.8
E. coli O157:H7 SALOD	4.0E+01	-81.2	-52.1	-108.2	-88.1
	4.0E+02	-26.8	-18.8	-71.4	-13.4
	4.0E+03	52.5	24.3	30.1	3.5

TABLE 22. The Limit of Detection of Two Capture Matrices Using RAPTOR Analysis (Continued)

		Strept-Biotin	Strept-Biotin	HSA-PG	HSA-PG
Baseline Signals	Baseline 1	479.5	454.9	501.8	579.9
	Baseline 2	504.5	478.0	562.7	607.6
	Baseline 3	534.7	503.6	617.4	630.7
	Baseline 4	570.1	521.6	665.4	649.7
Normalization Coefficients	B1/**LC** = B1N	1.1	1.0	1.1	1.3
	B2/**LC** = B2N	1.1	1.0	1.2	1.3
	B3/**LC** = B3N	1.1	1.0	1.2	1.3
	B4/**LC** = B4N	1.1	1.0	1.3	1.2
Normalized Baselines	B1/ B4N	438.7	454.9	393.4	465.6
	B2/B4N	461.6	478.0	441.1	487.8
	B3/B4N	489.2	503.6	484.0	506.3
	B4/B4N	521.6	521.6	521.6	521.6
	Average	477.8	489.5	460.0	495.3
	STDEV	35.8	29.2	55.3	24.2
	%CoV	7.5	6.0	12.0	4.9
E. coli O157:H7 Signals	10^-6	600.8	543.6	664.4	668.7
	10^-5	653.4	568.3	735.1	693.8
	10^-4	2008.6	1467.8	2447.5	1803.3
Normalized Ec Signals	10^-6/B4N	549.7	543.6	520.8	536.9
	10^-5/B4N	597.8	568.3	576.2	557.0
	10^-4/B4N	1837.7	1467.8	1918.6	1447.7
Limit of Detection	LOD	585.1	577.1	625.9	567.9
E. coli O157:H7 SALOD	1.3E+02	-35.4	-33.5	-105.0	-31.0
	1.3E+03	12.7	-8.8	-49.6	-10.9
	1.3E+06	1252.6	890.7	1292.7	879.9

		HSA-PG	HSA-PG	Strept-Biotin	Strept-Biotin
Baseline Signals	Baseline 1	645.8	613.9	558	434.6
	Baseline 2	660.5	627.2	567	450.8
	Baseline 3	661	636.1	569.5	456
	Baseline 4	672.5	652	577	466
Normalization Coefficients	B1/**LC** = B1N	1.5	1.4	1.3	1.0
	B2/**LC** = B2N	1.5	1.4	1.3	1.0
	B3/**LC** = B3N	1.4	1.4	1.2	1.0
	B4/**LC** = B4N	1.4	1.4	1.2	1.0
Normalized Baselines	B1/ B4N	447.5	438.8	450.7	434.6
	B2/B4N	457.7	448.3	457.9	450.8
	B3/B4N	458.0	454.6	459.9	456.0
	B4/B4N	466.0	466.0	466.0	466.0
	Average	457.3	451.9	458.6	451.9
	STDEV	7.6	11.4	6.3	13.1
	%CoV	1.7	2.5	1.4	2.9
E. coli O157:H7 Signals	10^-6	761.7	685.2	581.8	478.8
	10^-5	802.7	702.3	621	492.9
	10^-4	862.7	721.1	641.2	521.9
Normalized Ec Signals	10^-6/B4N	527.8	489.7	469.9	478.8
	10^-5/B4N	556.2	502.0	501.5	492.9
	10^-4/B4N	597.8	515.4	517.8	521.9
Limit of Detection	LOD	480.0	486.2	477.6	491.2
E. coli O157:H7 SALOD	2.1E+02	47.8	3.5	-7.7	-12.4
	2.1E+03	76.2	15.7	23.9	1.7
	2.1E+04	117.7	29.2	40.2	30.7

TABLE 22. The Limit of Detection of Two Capture Matrices Using RAPTOR Analysis (Continued)

		Strept-Biotin	Strept-Biotin	HSA-PG	HSA-PG
Baseline Signals	Baseline 1	672.7	584.7	576.1	402.8
	Baseline 2	703.4	594.4	617.9	433.6
	Baseline 3	731.0	612.9	641.7	465.5
	Baseline 4	763.8	623.1	675.8	489.6
Normalization Coefficients	B1/**LC** = B1N	1.7	1.5	1.4	1.0
	B2/**LC** = B2N	1.6	1.4	1.4	1.0
	B3/**LC** = B3N	1.6	1.3	1.4	1.0
	B4/**LC** = B4N	1.6	1.3	1.4	1.0
Normalized Baselines	B1/ B4N	431.2	459.4	417.4	402.8
	B2/B4N	450.9	467.0	447.7	433.6
	B3/B4N	468.6	481.6	464.9	465.5
	B4/B4N	489.6	489.6	489.6	489.6
	Average	460.1	474.4	454.9	447.9
	STDEV	24.9	13.7	30.4	37.8
	%CoV	5.4	2.9	6.7	8.4
E. coli O157:H7 Signals	10^-5	796.0	637.5	721.2	519.8
	10^-4	860.1	671.9	765.6	546.0
	10^-3	1286.5	956.0	1050.0	782.6
Normalized Ec Signals	10^-5/B4N	510.2	500.9	522.5	519.8
	10^-4/B4N	551.3	527.9	554.7	546.0
	10^-3/B4N	824.7	751.2	760.7	782.6
Limit of Detection	LOD	534.8	515.4	546.0	561.3
E. coli O157:H7 SALOD	1.0E+02	-24.6	-14.5	-23.5	-41.5
	1.0E+03	16.5	12.5	8.7	-15.3
	1.0E+04	289.8	235.7	214.7	221.3

		HSA-PG	HSA-PG	Strept-Biotin	Strept-Biotin
Baseline Signals	Baseline 1	618.0	519.0	615.4	476.2
	Baseline 2	636.7	502.6	657.2	463.4
	Baseline 3	668.0	506.7	694.9	479.8
	Baseline 4	695.5	525.7	739.8	491.1
Normalization Coefficients	B1/**LC** = B1N	1.3	1.1	1.3	1.0
	B2/**LC** = B2N	1.4	1.1	1.4	1.0
	B3/**LC** = B3N	1.4	1.1	1.4	1.0
	B4/**LC** = B4N	1.4	1.1	1.5	1.0
Normalized Baselines	B1/ B4N	436.4	484.8	408.5	476.2
	B2/B4N	449.6	469.5	436.3	463.4
	B3/B4N	471.7	473.4	461.3	479.8
	B4/B4N	491.1	491.1	491.1	491.1
	Average	462.2	479.7	449.3	477.6
	STDEV	24.2	10.0	35.2	11.4
	%CoV	5.2	2.1	7.8	2.4
E. coli O157:H7 Signals	10^-5	722.6	546.7	759.9	522.9
	10^-4	742.4	554.9	813.6	559.4
	10^-3	1069.4	755.5	1163.6	804.1
	10^-2	3811.5	2678.5	4411.0	3091.0
	10^-1	6385.5	4378.0	7381.0	5340.5
Normalized Ec Signals	10^-5/B4N	510.2	510.7	504.4	522.9
	10^-4/B4N	524.2	518.4	540.1	559.4
	10^-3/B4N	755.1	705.8	772.4	804.1
	10^-2/B4N	2691.3	2502.2	2928.1	3091.0
	10^1/B4N	4508.9	4089.9	4899.7	5340.5
Limit of Detection	LOD	534.7	509.7	555.0	511.9
E. coli O157:H7 SALOD	1.0E+02	-24.4	1.0	-50.5	11.0
	1.0E+03	-10.5	8.7	-14.9	47.5
	1.0E+04	220.4	196.1	217.4	292.2
	1.0E+05	2156.7	1992.5	2373.2	2579.1
	1.0E+06	3974.2	3580.1	4344.7	4828.6

TABLE 23.The Limit of Detection in Ground Beef Homogenate Supernatant Fluid

		HSA-PG	HSA-PG	HSA-PG	HSA-PG
Baseline Signals	Baseline 1	474.7	397.5	322.6	301.4
	Baseline 2	498.2	321.5	367.0	363.8
	Baseline 3	456.1	394.0	325.2	345.4
	Baseline 4	465.4	372.0	301.5	315.6
Normalization Coefficients	B1/LC = B1N	1.6	1.3	1.1	1.0
	B2/LC = B2N	1.5	1.0	1.1	1.1
	B3/LC = B3N	1.4	1.2	1.0	1.1
	B4/LC = B4N	1.5	1.2	1.0	1.0
Normalized Baselines	B1/ B4N	307.5	322.2	322.6	287.9
	B2/B4N	322.7	260.6	367.0	347.5
	B3/B4N	295.5	319.3	325.2	330.0
	B4/B4N	301.5	301.5	301.5	301.5
	Average	306.8	300.9	329.1	316.7
	STDEV	11.7	28.4	27.4	27.0
	%CoV	3.8	9.4	8.3	8.5
E. coli O157:H7 Signals	10^-2	559.7	488.5	351.6	350.5
	10^-1	913.7	598.5	456.4	474.1
	10^0	1313.6	864.5	551.9	508.0
Normalized Ec Signals	10^-2/B4N	362.6	395.9	351.6	334.8
	10^-1/B4N	591.9	485.1	456.4	452.9
	10^0/B4N	851.0	700.7	551.9	485.3
Limit of Detection E. coli O157:H7 SALOD	LOD	341.9	386.1	411.3	397.7
	5.7E+04	20.7	9.8	-59.7	-62.9
	5.7E+05	250.0	99.0	45.1	55.2
	5.7E+06	509.1	314.6	140.6	87.6
		Strept-Biotin	Strept-Biotin	HSA-PG	HSA-PG
Baseline Signals	Baseline 1	380.6	337.0	339.1	351.0
	Baseline 2	335.3	280.5	336.1	321.2
	Baseline 3	319.1	257.0	295.8	300.2
	Baseline 4	306.6	270.3	292.2	299.2
Normalization Coefficients	B1/LC = B1N	1.1	1.0	1.0	1.0
	B2/LC = B2N	1.2	1.0	1.2	1.1
	B3/LC = B3N	1.2	1.0	1.2	1.2
	B4/LC = B4N	1.1	1.0	1.1	1.1
Normalized Baselines	B1/ B4N	335.5	337.0	313.7	317.1
	B2/B4N	295.6	280.5	310.9	290.2
	B3/B4N	281.3	257.0	273.6	271.2
	B4/B4N	270.3	270.3	270.3	270.3
	Average	295.7	286.2	292.1	287.2
	STDEV	28.5	35.2	23.4	21.9
	%CoV	9.6	12.3	8.0	7.6
E. coli O157:H7 Signals	10^-2	366.5	396.5	352.1	346.9
	10^-1	646.6	815.5	646.3	664.0
	10^0	835.1	850.9	726.3	855.0
Normalized Ec Signals	10^-2/B4N	323.1	396.5	325.7	313.4
	10^-1/B4N	570.0	815.5	597.9	599.9
	10^0/B4N	736.2	850.9	671.9	772.4
Limit of Detection E. coli O157:H7 SALOD	LOD	381.2	391.8	362.2	353.0
	5.4E+05	-58.1	4.7	-36.5	-39.6
	5.4E+06	188.8	423.7	235.7	246.8
	5.4E+07	355.0	459.1	309.7	419.4

TABLE 23. The Limit of Detection in Ground Beef Homogenate Supernatant Fluid

		Strept-Biotin	Strept-Biotin	HSA-PG	HSA-PG
Baseline Signals	Baseline 1	323.8	453.9	331.9	330.5
	Baseline 2	305.1	553.0	296.3	315.1
	Baseline 3	307.7	605.0	288.6	316.1
	Baseline 4	316.0	662.5	298.9	314.1
Normalization Coefficients	B1/LC = B1N	1.0	1.4	1.0	1.0
	B2/LC = B2N	1.0	1.9	1.0	1.1
	B3/LC = B3N	1.1	2.1	1.0	1.1
	B4/LC = B4N	1.1	2.2	1.0	1.1
Normalized Baselines	B1/ B4N	306.3	204.8	331.9	314.5
	B2/B4N	288.6	249.5	296.3	299.9
	B3/B4N	291.0	273.0	288.6	300.8
	B4/B4N	298.9	298.9	298.9	298.9
	Average	296.2	256.5	303.9	303.5
	STDEV	8.0	40.0	19.2	7.4
	%CoV	2.7	15.6	6.3	2.4
E. coli O157:H7 Signals	10^-2	390.5	693.0	323.7	357.1
	10^-1	853.8	1086.5	446.5	682.0
	10^0	1621.2	2254.5	617.9	873.9
Normalized Ec Signals	10^-2/B4N	369.4	312.7	323.7	339.8
	10^-1/B4N	807.6	490.2	446.5	649.0
	10^0/B4N	1533.5	1017.2	617.9	831.6
Limit of Detection	LOD	320.3	376.4	361.4	325.6
E. coli O157:H7 SALOD	1.5E+05	49.1	-63.8	-37.7	14.2
	1.5E+06	487.3	113.8	85.1	323.4
	1.5E+07	1213.2	640.7	256.5	506.0

TABLE 24. The Limit of Detection in Spinach Homogenate Supernatant Fluid

		HSA-PG	HSA-PG	HSA-PG	HSA-PG
Baseline Signals	Baseline 1	891.3	929.8	844.0	805.2
	Baseline 2	1163.1	1028.3	1036.1	1142.3
	Baseline 3	1349.5	1056.5	1149.1	1242.9
	Baseline 4	1518.2	989.9	1195.1	1308.1
Normalization Coefficients	B1/LC = B1N	1.1	1.2	1.0	1.0
	B2/LC = B2N	1.1	1.0	1.0	1.1
	B3/LC = B3N	1.3	1.0	1.1	1.2
	B4/LC = B4N	1.5	1.0	1.2	1.3
Normalized Baselines	B1/ B4N	581.1	929.8	699.1	609.3
	B2/B4N	758.4	1028.3	858.2	864.4
	B3/B4N	879.9	1056.5	951.8	940.6
	B4/B4N	989.9	989.9	989.9	989.9
	Average	802.3	1001.1	874.7	851.1
	STDEV	175.2	54.8	129.5	169.2
	%CoV	21.8	5.5	14.8	19.9
E. coli O157:H7 Signals	10^-2	2077.3	1313.5	1647.3	1657.0
	10^-1	4603.5	2123.0	4312.0	3415.5
	10^0	4785.0	3096.5	4862.0	3525.5
Normalized Ec Signals	10^-2/B4N	1354.4	1313.5	1364.5	1253.9
	10^-1/B4N	3001.6	2123.0	3571.6	2584.7
	10^0/B4N	3119.9	3096.5	4027.2	2667.9
Limit of Detection	LOD	1327.8	1165.6	1263.3	1358.7
E. coli O157:H7 SALOD	2.9E+05	26.6	147.9	101.1	-104.8
	2.9E+06	1673.7	957.4	2308.3	1226.0
	2.9E+07	1792.1	1930.9	2763.9	1309.2

TABLE 25. Cells Capture on Waveguide Surface, Capture Efficiency

		HSA-PG	Strept-Biotin	Strept-Biotin	HSA-PG
Baseline Signals	Baseline 1	502.9	346.2	375.8	429.5
	Baseline 2	533.1	378	458.9	449.5
	Baseline 3	602.9	387.7	516.8	462.4
	Baseline 4	633.6	407.7	552.4	478.8
Normalization Coefficients	B1/LC = B1N	1.5	1.0	1.1	1.2
	B2/LC = B2N	1.4	1.0	1.2	1.2
	B3/LC = B3N	1.6	1.0	1.3	1.2
	B4/LC = B4N	1.6	1.0	1.4	1.2
Normalized Baselines	B1/ B4N	323.6	346.2	277.4	365.7
	B2/B4N	343.0	378.0	338.7	382.8
	B3/B4N	387.9	387.7	381.4	393.7
	B4/B4N	407.7	407.7	407.7	407.7
	Average	365.6	379.9	351.3	387.5
	STDEV	38.9	25.6	56.9	17.7
	%CoV	10.6	6.8	16.2	4.6
E. coli O157:H7 Signals	10^0	2288	1323.7	1837.3	1513.8
Normalized Ec Signals	10^0	1472.3	1323.7	1356.0	1289.0
Limit of Detection	LOD	482.3	456.8	522.0	440.7
E. coli O157:H7 SALOD	1.7E+08	989.9	866.9	834.0	848.3

		HSA-PG	HSA-PG	Strept-Biotin	Strept-Biotin
Baseline Signals	Baseline 1	657.5	547.2	690.2	673.8
	Baseline 2	783	626.2	995.3	824.7
	Baseline 3	887.6	705.7	1205.4	1002.7
	Baseline 4	885.5	760.1	1358.7	1038.7
Normalization Coefficients	B1/LC = B1N	1.2	1.0	1.3	1.2
	B2/LC = B2N	1.3	1.0	1.6	1.3
	B3/LC = B3N	1.3	1.0	1.7	1.4
	B4/LC = B4N	1.2	1.0	1.8	1.4
Normalized Baselines	B1/ B4N	564.4	547.2	386.1	493.1
	B2/B4N	672.1	626.2	556.8	603.5
	B3/B4N	761.9	705.7	674.3	733.8
	B4/B4N	760.1	760.1	760.1	760.1
	Average	689.6	659.8	594.3	647.6
	STDEV	93.4	93.0	161.9	123.7
	%CoV	13.5	14.1	27.2	19.1
E. coli O157:H7 Signals	10^-1	3246	2315.5	4559.5	2904
Normalized Ec Signals	10^-1	2786.3	2315.5	2550.7	2125.1
Limit of Detection	LOD	969.9	938.9	1080.1	1018.7
E. coli O157:H7 SALOD	1.7E+07	1816.4	1376.6	1470.7	1106.4

TABLE 25. Cells Capture on Waveguide Surface, Capture Efficiency (Continued)

		HSA-PG	Strept-Biotin	Strept-Biotin	HSA-PG
Baseline Signals	Baseline 1	345.2	344.1	343.8	389.0
	Baseline 2	580.5	388.2	421.8	536.3
	Baseline 3	652.9	419.0	470.8	603.0
	Baseline 4	737.2	443.6	511.6	648.7
Normalization Coefficients	B1/LC = B1N	1.0	1.0	1.0	1.1
	B2/LC = B2N	1.5	1.0	1.1	1.4
	B3/LC = B3N	1.6	1.0	1.1	1.4
	B4/LC = B4N	1.7	1.0	1.2	1.5
Normalized Baselines	B1/ B4N	207.7	344.1	298.1	266.0
	B2/B4N	349.3	388.2	365.7	366.7
	B3/B4N	392.9	419.0	408.2	412.3
	B4/B4N	443.6	443.6	443.6	443.6
	Average	348.4	398.7	378.9	372.2
	STDEV	101.4	42.9	62.6	77.5
	%CoV	29.1	10.8	16.5	20.8
E. coli O157:H7 Signals	10^0	2000.8	1549.4	2073.7	1037.1
Normalized Ec Signals	10^0	1204.0	1549.4	1798.1	709.2
Limit of Detection	LOD	652.5	527.4	566.6	604.7
E. coli O157:H7 SALOD	4.3E+08	551.4	1022.0	1231.4	104.5
		Strept-Biotin	Strept-Biotin	HSA-PG	HSA-PG
Baseline Signals	Baseline 1	441	362.1	373.2	498.3
	Baseline 2	475.9	389.8	404.7	644.4
	Baseline 3	517	412.9	420.2	663.7
	Baseline 4	529.5	431.3	444.5	693.3
Normalization Coefficients	B1/LC = B1N	1.2	1.0	1.0	1.4
	B2/LC = B2N	1.2	1.0	1.0	1.7
	B3/LC = B3N	1.3	1.0	1.0	1.6
	B4/LC = B4N	1.2	1.0	1.0	1.6
Normalized Baselines	B1/ B4N	359.2	362.1	362.1	310.0
	B2/B4N	387.6	389.8	392.7	400.9
	B3/B4N	421.1	412.9	407.7	412.9
	B4/B4N	431.3	431.3	431.3	431.3
	Average	399.8	399.0	398.5	388.8
	STDEV	32.9	29.9	29.0	54.0
	%CoV	8.2	7.5	7.3	13.9
E. coli O157:H7 Signals	10^-1	2172.5	1622.7	2568.5	3575.7
Normalized Ec Signals	10^-1	1769.6	1622.7	2492.2	2224.4
Limit of Detection	LOD	498.4	488.7	485.4	550.7
E. coli O157:H7 SALOD	2.8E+07	1271.2	1134.0	2006.8	1673.7

TABLE 25. Cells Capture on Waveguide Surface, Capture Efficiency (Continued)

		Strept-Biotin	HSA-PG	HSA-PG	Strept-Biotin
Baseline Signals	Baseline 1	470.6	422.1	464.1	459.3
	Baseline 2	492.5	432.4	497.6	481.9
	Baseline 3	510.2	442.6	535.3	516.8
	Baseline 4	530	456.5	568.4	540.9
Normalization Coefficients	B1/LC = B1N	1.1	1.0	1.1	1.1
	B2/LC = B2N	1.1	1.0	1.2	1.1
	B3/LC = B3N	1.2	1.0	1.2	1.2
	B4/LC = B4N	1.2	1.0	1.2	1.2
Normalized Baselines	B1/ B4N	405.3	422.1	372.7	387.6
	B2/B4N	424.2	432.4	399.6	406.7
	B3/B4N	439.4	442.6	429.9	436.2
	B4/B4N	456.5	456.5	456.5	456.5
	Average	431.4	438.4	414.7	421.7
	STDEV	21.8	14.7	36.4	30.6
	%CoV	5.1	3.3	8.8	7.3
E. coli O157:H7 Signals	10^-2	2114.8	2234.1	2867.5	2222
Normalized Ec Signals	10^-2	1821.5	2234.1	2303.0	1875.3
Limit of Detection	LOD	496.8	482.5	523.8	513.5
E. coli O157:H7 SALOD	1.1E+06	1324.7	1751.6	1779.2	1361.8
		Strept-Biotin	HSA-PG	HSA-PG	Strept-Biotin
Baseline Signals	Baseline 1	467	371.8	356.7	394.1
	Baseline 2	518	422.6	409.9	490.6
	Baseline 3	550.8	447.7	457.9	502.9
	Baseline 4	565.4	446.7	485.8	544.5
Normalization Coefficients	B1/LC = B1N	1.3	1.0	1.0	1.1
	B2/LC = B2N	1.3	1.0	1.0	1.2
	B3/LC = B3N	1.2	1.0	1.0	1.1
	B4/LC = B4N	1.3	1.0	1.1	1.2
Normalized Baselines	B1/ B4N	369.0	371.8	328.0	323.3
	B2/B4N	409.3	422.6	376.9	402.5
	B3/B4N	435.2	447.7	421.0	412.6
	B4/B4N	446.7	446.7	446.7	446.7
	Average	415.0	422.2	393.2	396.3
	STDEV	34.5	35.5	52.1	52.2
	%CoV	8.3	8.4	13.3	13.2
E. coli O157:H7 Signals	10^0	2821.5	1475	1537.8	1538
Normalized Ec Signals	10^0	2229.2	1475.0	1414.0	1261.8
Limit of Detection	LOD	518.4	528.8	549.6	552.8
E. coli O157:H7 SALOD	1.8E+08	1710.7	946.2	864.5	708.9

TABLE 25. Cells Capture on Waveguide Surface, Capture Efficiency (Continued)

		HSA-PG	Strept-Biotin	Strept-Biotin	HSA-PG
Baseline Signals	Baseline 1	647.1	404.6	538.4	530.1
	Baseline 2	693.5	422.6	593.2	549.6
	Baseline 3	741.4	453.9	624.1	584
	Baseline 4	762.7	463.1	639.1	607.1
Normalization Coefficients	B1/LC = B1N	1.6	1.0	1.3	1.3
	B2/LC = B2N	1.6	1.0	1.4	1.3
	B3/LC = B3N	1.6	1.0	1.4	1.3
	B4/LC = B4N	1.6	1.0	1.4	1.3
Normalized Baselines	B1/ B4N	392.9	404.6	390.1	404.4
	B2/B4N	421.1	422.6	429.8	419.2
	B3/B4N	450.2	453.9	452.2	445.5
	B4/B4N	463.1	463.1	463.1	463.1
	Average	431.8	436.1	433.8	433.0
	STDEV	31.3	27.2	32.3	26.3
	%CoV	7.3	6.2	7.4	6.1
E. coli O157:H7 Signals	10^-1	6583.5	3657.5	5626.5	4653
Normalized Ec Signals	10^-1	3997.4	3657.5	4077.0	3549.3
Limit of Detection	LOD	525.8	517.7	530.6	511.9
E. coli O157:H7 SALOD	7.8E+07	3471.6	3139.8	3546.4	3037.5

		HSA-PG	HSA-PG	Strept-Biotin	Strept-Biotin
Baseline Signals	Baseline 1	594	503.6	478.5	449
	Baseline 2	613.8	533.9	503.3	474.1
	Baseline 3	653.4	562.6	519.3	490.6
	Baseline 4	679.4	587.2	526	503.9
Normalization Coefficients	B1/LC = B1N	1.3	1.1	1.1	1.0
	B2/LC = B2N	1.3	1.1	1.1	1.0
	B3/LC = B3N	1.3	1.1	1.1	1.0
	B4/LC = B4N	1.3	1.2	1.0	1.0
Normalized Baselines	B1/ B4N	440.6	432.2	458.4	449.0
	B2/B4N	455.2	458.2	482.2	474.1
	B3/B4N	484.6	482.8	497.5	490.6
	B4/B4N	503.9	503.9	503.9	503.9
	Average	471.1	469.3	485.5	479.4
	STDEV	28.5	31.0	20.2	23.6
	%CoV	6.1	6.6	4.2	4.9
E. coli O157:H7 Signals	10^-2	4240.5	2832.5	3388	3080
Normalized Ec Signals	10^-2	3145.1	2430.7	3245.7	3080.0
Limit of Detection	LOD	556.7	562.2	546.2	550.3
E. coli O157:H7 SALOD	1.1E+06	2588.4	1868.4	2699.5	2529.7

TABLE 26. A Comparison of DyLight™649 and Cy5

		DyLight	Cy5	Cy5	DyLight	Cy5	DyLight	DyLight	Cy5
Baseline Signals	Baseline 1	916.3	541.6	465.1	587	3230.5	542.1	750.6	1742.7
	Baseline 2	1029.8	575.4	488.4	634.8	3377.0	585.7	764.0	1742.2
	Baseline 3	1127.2	600.6	519.3	689.2	3899.5	592.4	798.6	1764.3
	Baseline 4	1202.7	632.4	549.8	724.6	3993.0	611.9	819.3	1776.6
Normalization Coefficients	B1/LC = B1N	1.7	1.0	0.9	1.1	6.0	1.0	1.4	3.2
	B2/LC = B2N	1.8	1.0	0.8	1.1	5.8	1.0	1.3	3.0
	B3/LC = B3N	1.9	1.0	0.9	1.1	6.6	1.0	1.3	3.0
	B4/LC = B4N	1.9	1.0	0.9	1.1	6.5	1.0	1.3	2.9
Normalized Baselines	B1/ B4N	481.8	541.6	535.0	512.3	495.1	542.1	560.6	600.2
	B2/B4N	541.5	575.4	561.8	554.0	517.5	585.7	570.6	600.1
	B3/B4N	592.7	600.6	597.3	601.5	597.6	592.4	596.4	607.7
	B4/B4N	632.4	632.4	632.4	632.4	611.9	611.9	611.9	611.9
	Average	562.1	587.5	581.6	575.1	555.5	583.0	584.9	605.0
	STDEV	65.2	38.5	42.4	52.8	57.9	29.5	23.5	5.8
	%CoV	11.6	6.5	7.3	9.2	10.4	5.1	4.0	1.0
E. coli O157:H7 Signals	10^-6	1287	659	583.3	768.7	3212.0	620.6	852.8	1817.7
	10^-5	1357.3	703.2	615.9	805.2	3932.5	643.7	906.0	1804.8
	10^-4	1477.6	761.6	691.2	887.3	4020.5	716.0	975.7	1849.0
Normalized Ec Signals	10^-6/B4N	676.7	659.0	670.9	670.9	492.2	620.6	636.9	626.1
	10^-5/B4N	713.7	703.2	708.4	702.7	602.6	643.7	676.7	621.6
	10^-4/B4N	776.9	761.6	795.0	774.4	616.1	716.0	728.7	636.8
Limit of Detection	LOD	757.7	702.9	708.8	733.5	729.1	671.4	655.4	622.5
E. coli O157:H7 SALOD	6.0E+01	-81.0	-43.9	-37.9	-62.6	-236.9	-50.8	-18.5	3.6
	6.0E+02	-44.0	0.3	-0.4	-30.8	-126.5	-27.7	21.3	-0.8
	6.0E+03	19.3	58.7	86.2	40.9	-113.0	44.6	73.3	14.4